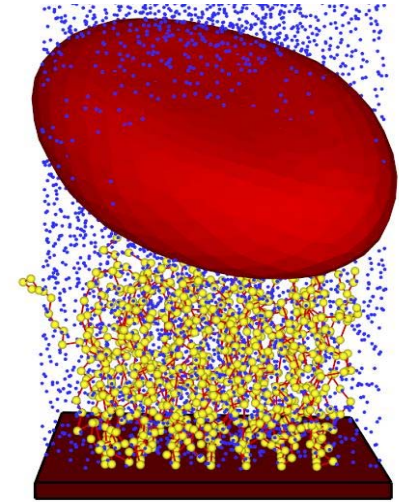
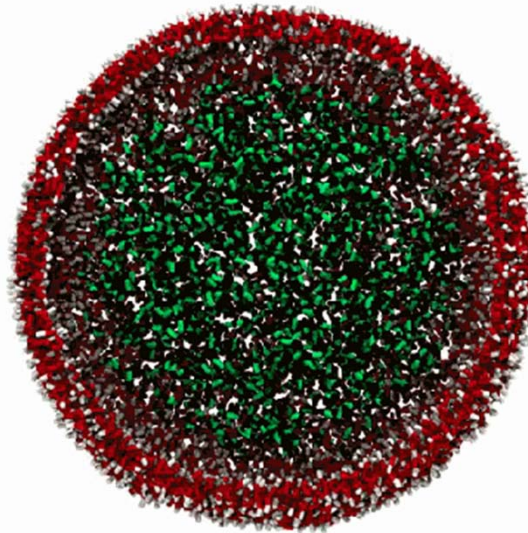
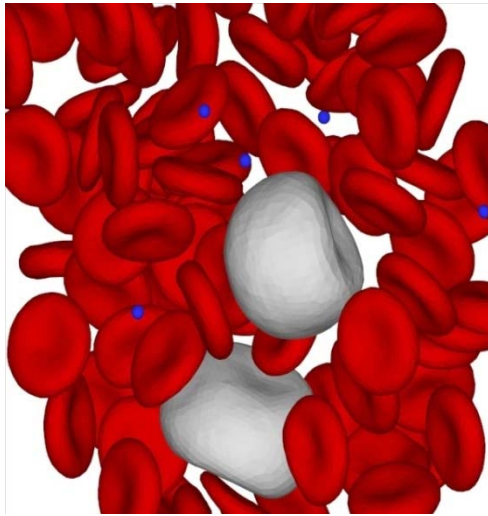


Dissipative Particle Dynamics:

Foundation, Evolution and Applications

Lecture 4: DPD in soft matter and polymeric applications



George Em Karniadakis

Division of Applied Mathematics, Brown University
& Department of Mechanical Engineering, MIT
& Pacific Northwest National Laboratory, CM4

The CRUNCH group: www.cfm.brown.edu/crunch

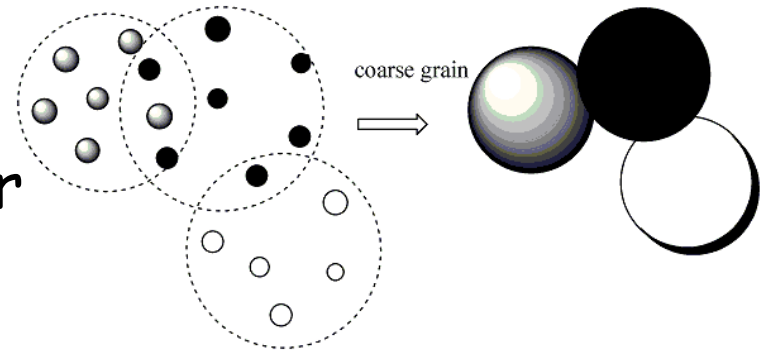


Outline

- ❖ Dissipative Particle Dynamics (DPD)
- ❖ Applications:
 - Fluid Flow
 - Boundary conditions
 - Triple-Decker: MD - DPD - NS
 - Blood Flow
 - Amphiphilic Self-assembly
- ❖ Future of DPD

Dissipative Particle Dynamics (DPD)

- Stochastic simulation approach for simple and complex fluids.
- Mesoscale approach to simulate soft matter.
- Conserve momentum locally & preserve hydrodynamics.
- Access to longer time and length scales than are possible using conventional MD simulations.

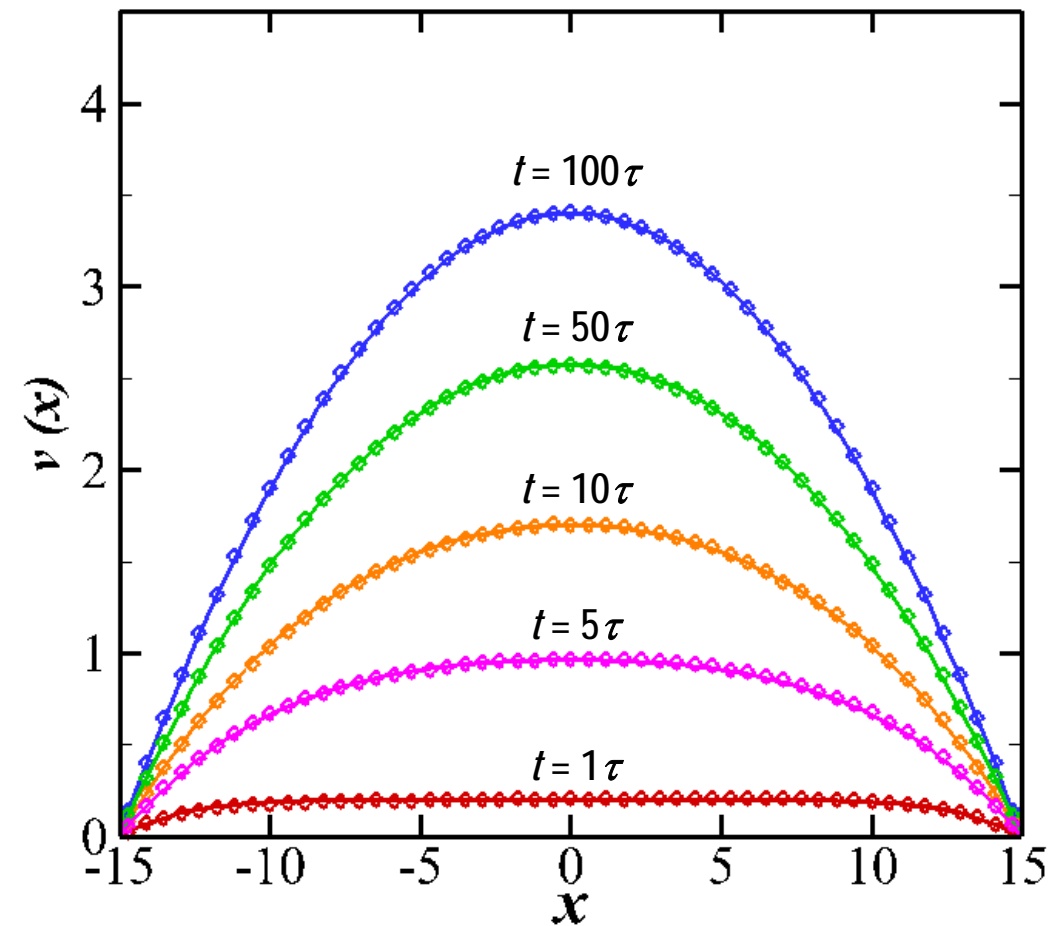
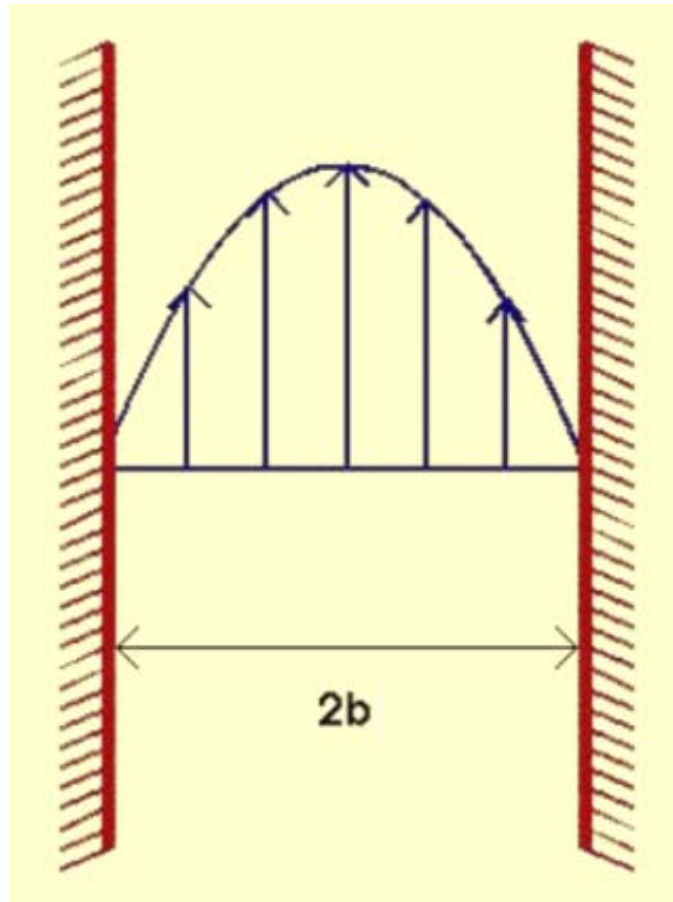


Simulations with DPD

- Applying appropriate boundary conditions, so we can simulate problems of interest.
- A choice for the inter-particle forces, so we can model materials of interest.
- DPD has been applied to model a diverse range of systems:
 - Fluid flow (pipes, porous media)
 - Complex fluids (Colloidal suspension, blood)
 - Self-assembly (polymers, lipids, surfactants, nanoparticles)
 - Phase phenomena (polymer melts, dynamic wetting)



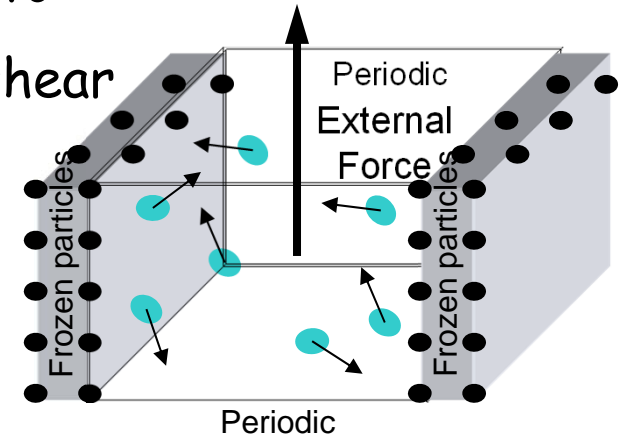
Fluid flow



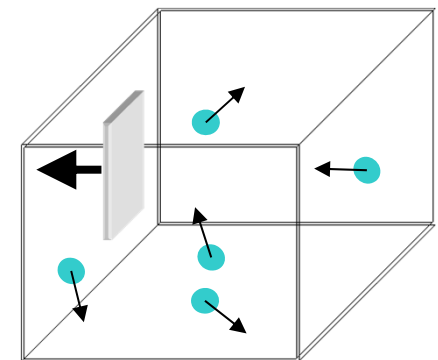
The development of velocity profiles in Poiseuille flow

Boundary Conditions in DPD

- Lees-Edwards boundary conditions can be used to simulate an infinite but periodic system under shear
- Revenga et al. (1998) created a solid boundary by freezing the particles on the boundary of solid object; no repulsion between the particles was used.



- Willemsen et al. (2000) used layers of ghost particles to generate no-slip boundary conditions.
- Pivkin & Karniadakis (2005) proposed new wall-fluid interaction forces.



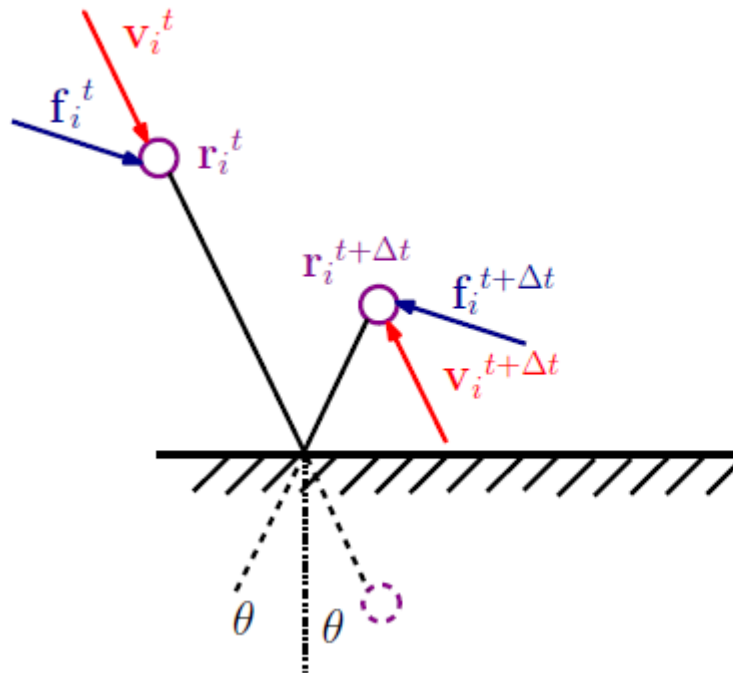
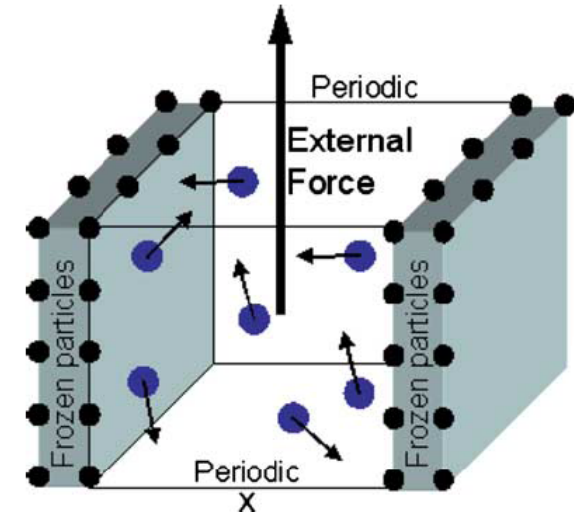
CRUNCH GROUP



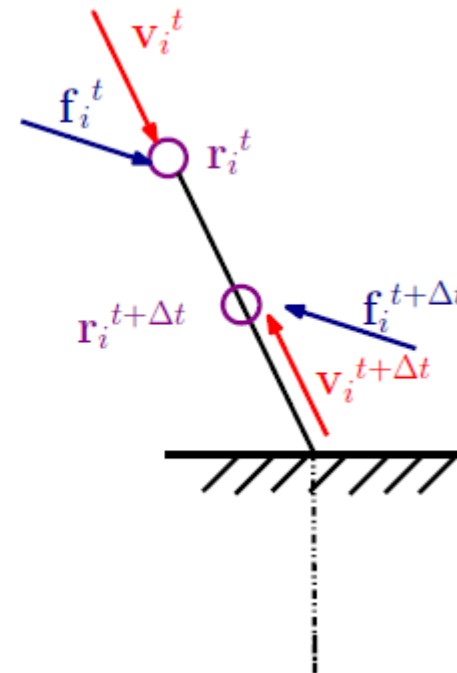
Boundary conditions in DPD

Frozen wall boundary condition

- Fluid in between parallel walls
- Walls are simulated by freezing DPD particles
- Flow induced by external body force

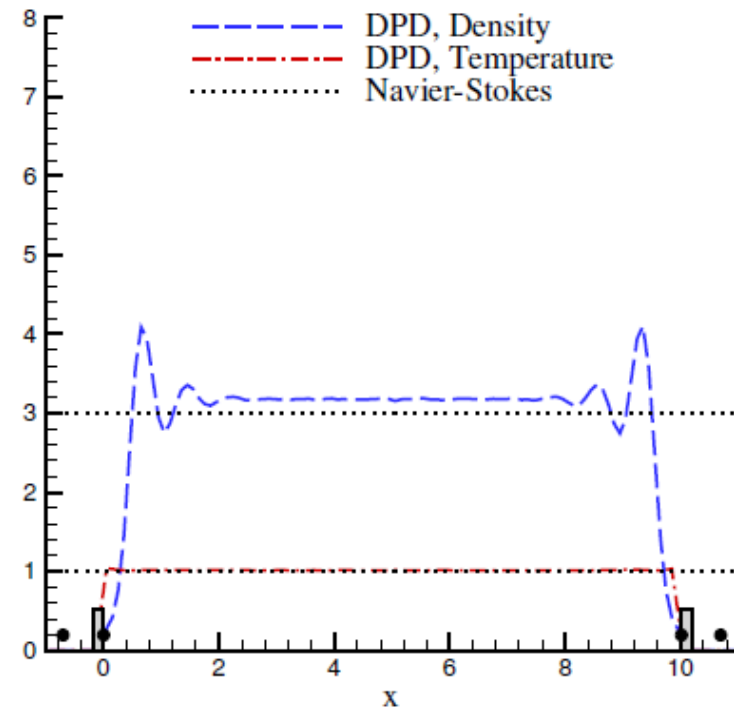
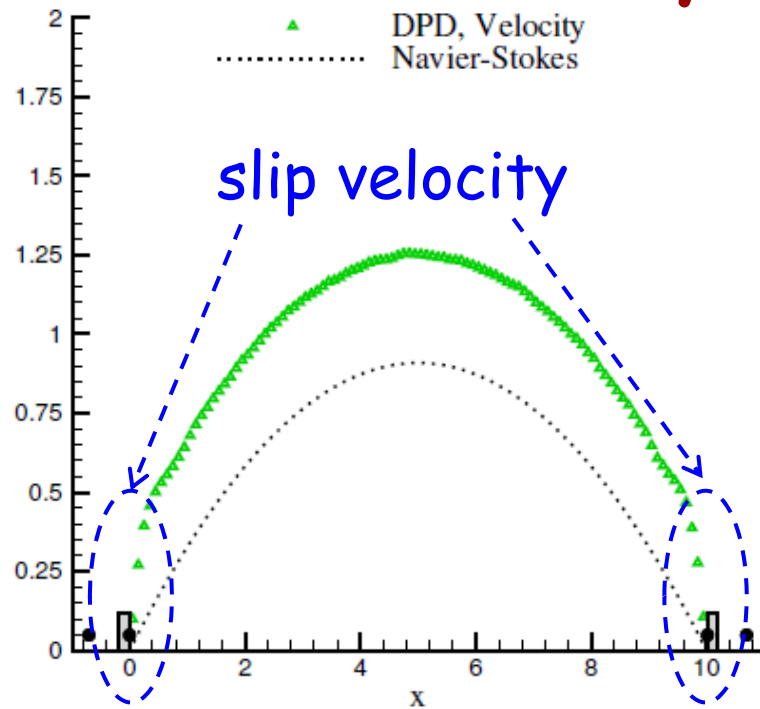


Bounce forward reflection

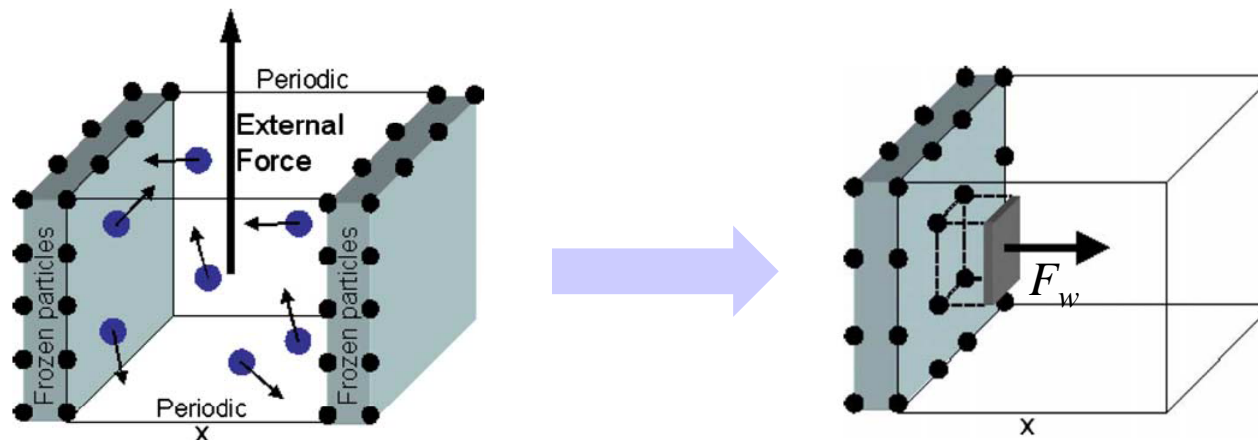


Bounce back reflection

Boundary conditions in DPD



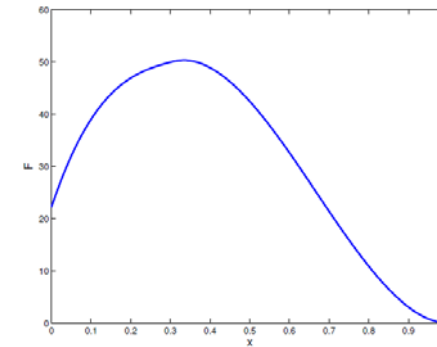
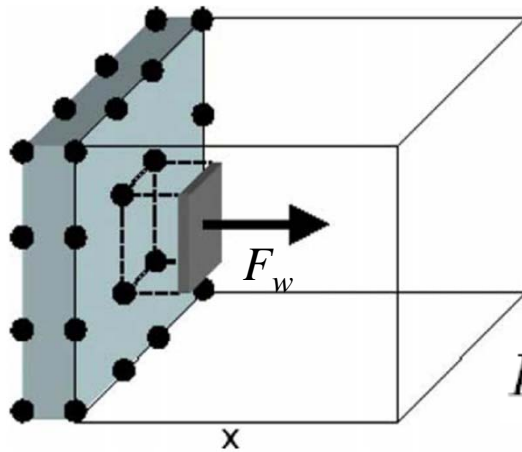
No-slip boundary condition



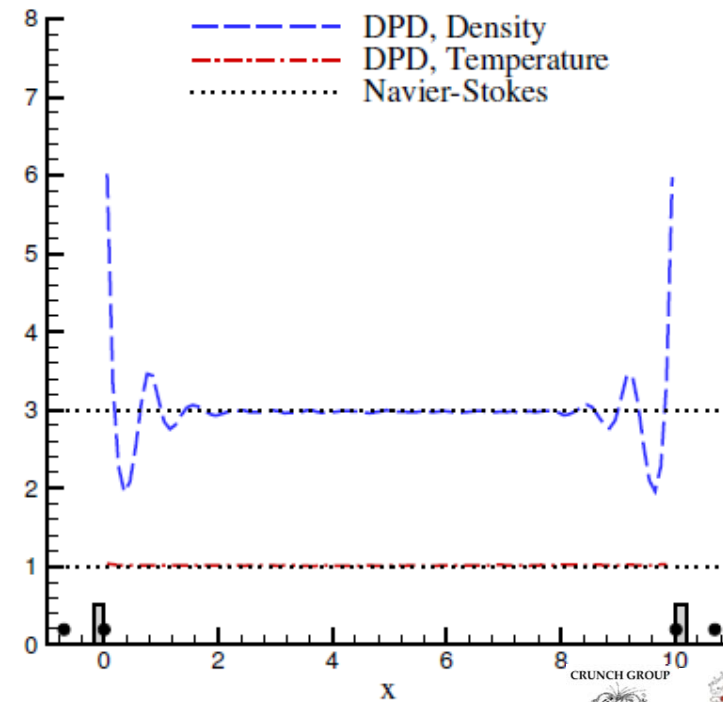
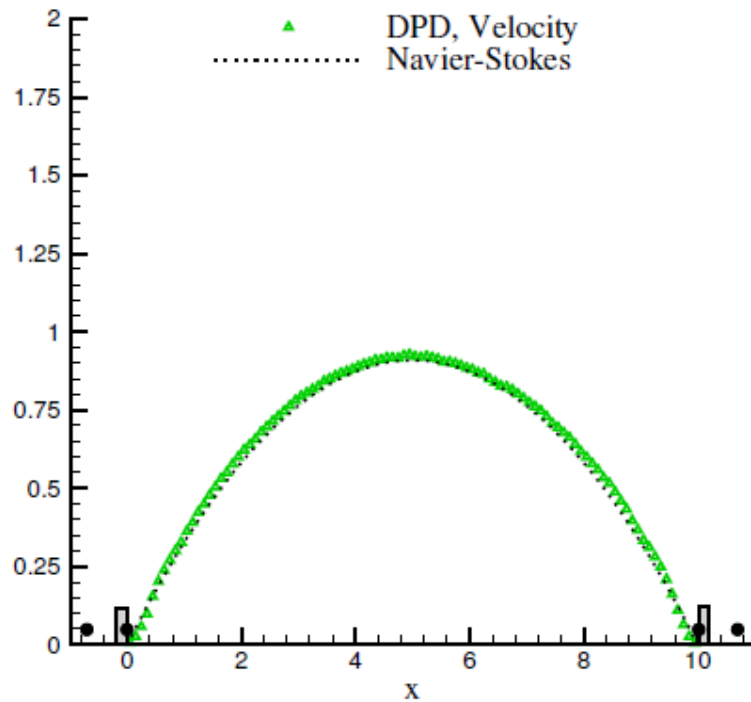
Pivkin & Karniadakis. J. Comput. Phys., 2005.



Poiseuille flow results



$$F_w = a_e(0.0303n_w^2 + 0.5617n_w - 0.8536)$$

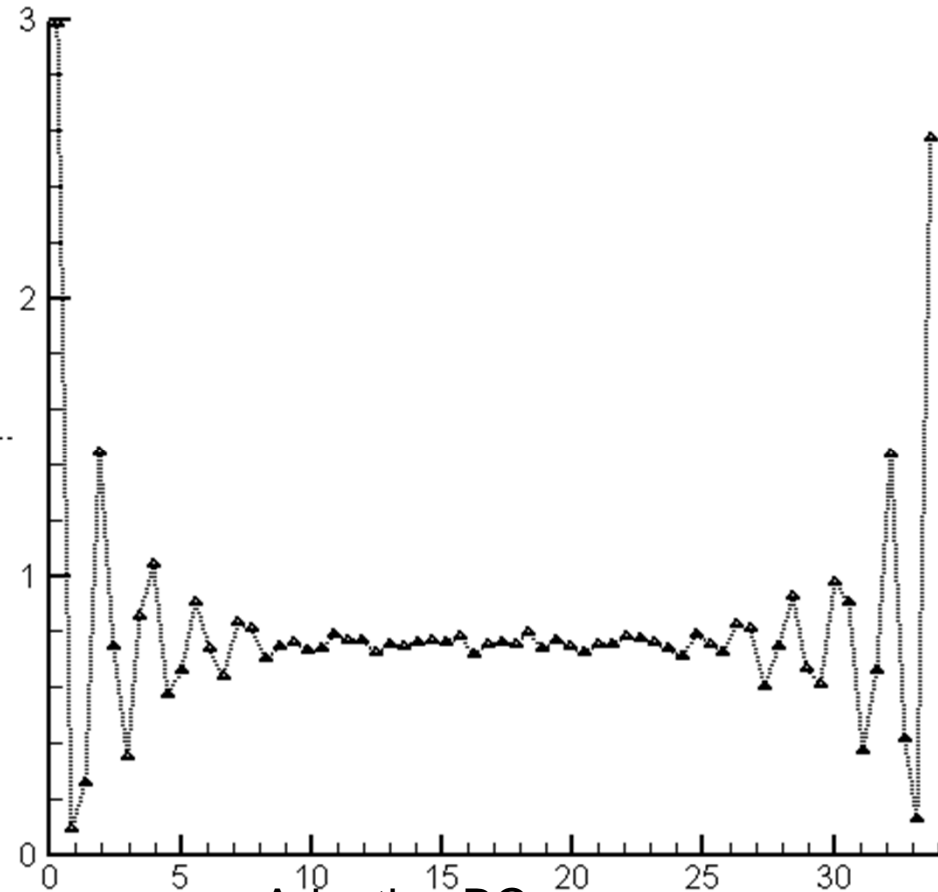
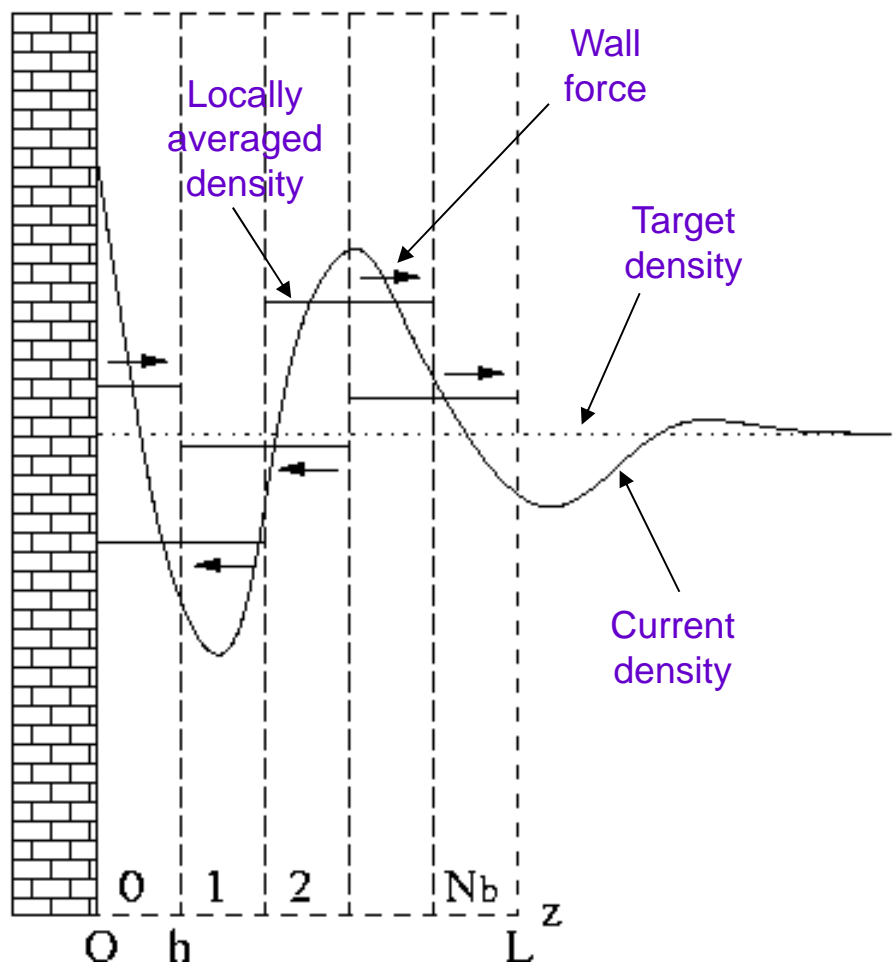


Pivkin & Karniadakis. J. Comput. Phys., 2005.



Boundary conditions in DPD

Adaptive boundary condition



Adaptive BC:

- layers of particles
- bounce back reflection
- **adaptive wall force**

Iteratively adjust the wall repulsion force in each bin based on the averaged density values.

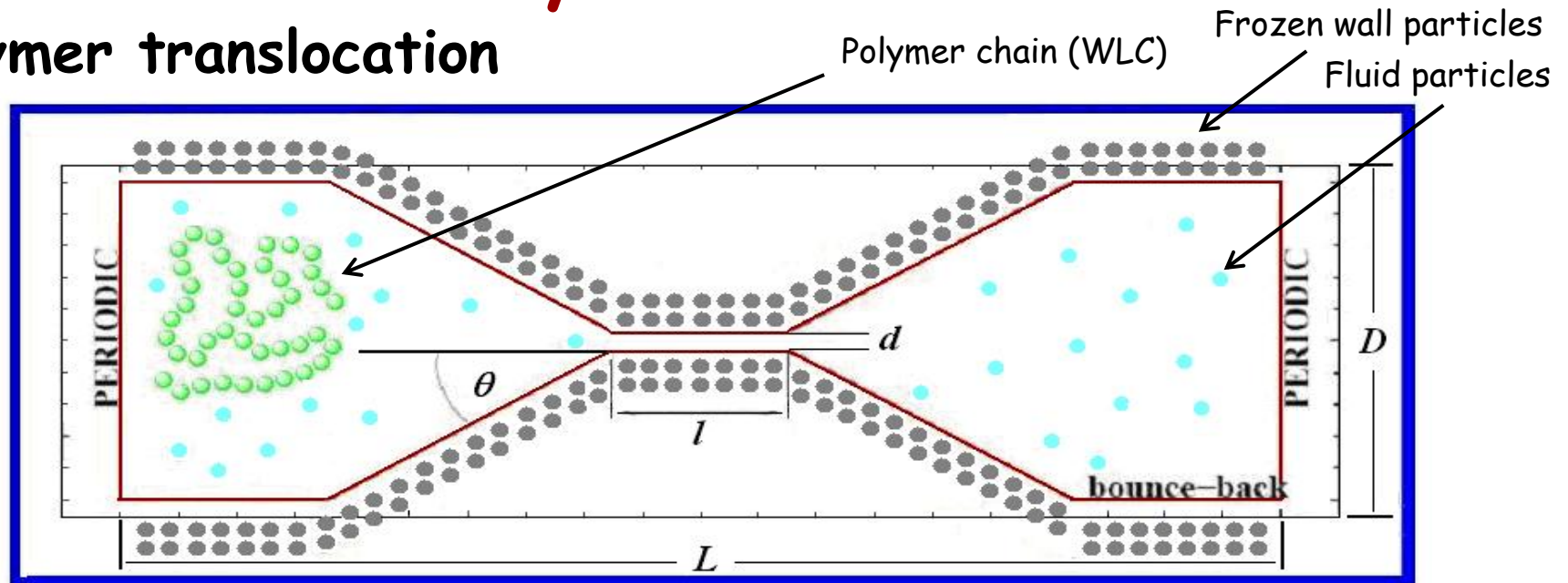
Pivkin & Karniadakis, PRL, 2006

CRUNCH GROUP



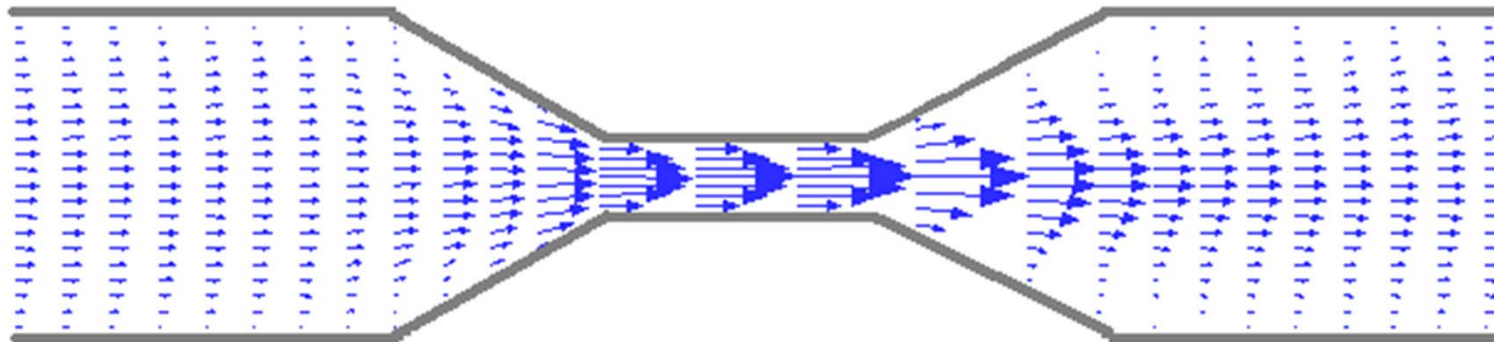
Boundary conditions in DPD

Polymer translocation



Schematic representation of simulation model

No-slip B.C. + Adaptive B.C.



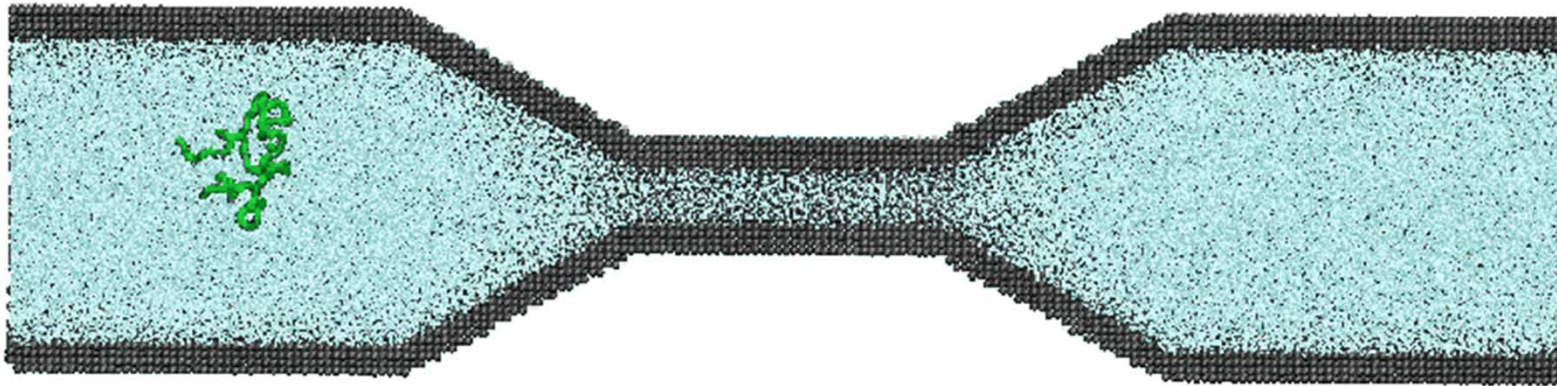
velocity vector field

CRUNCH GROUP

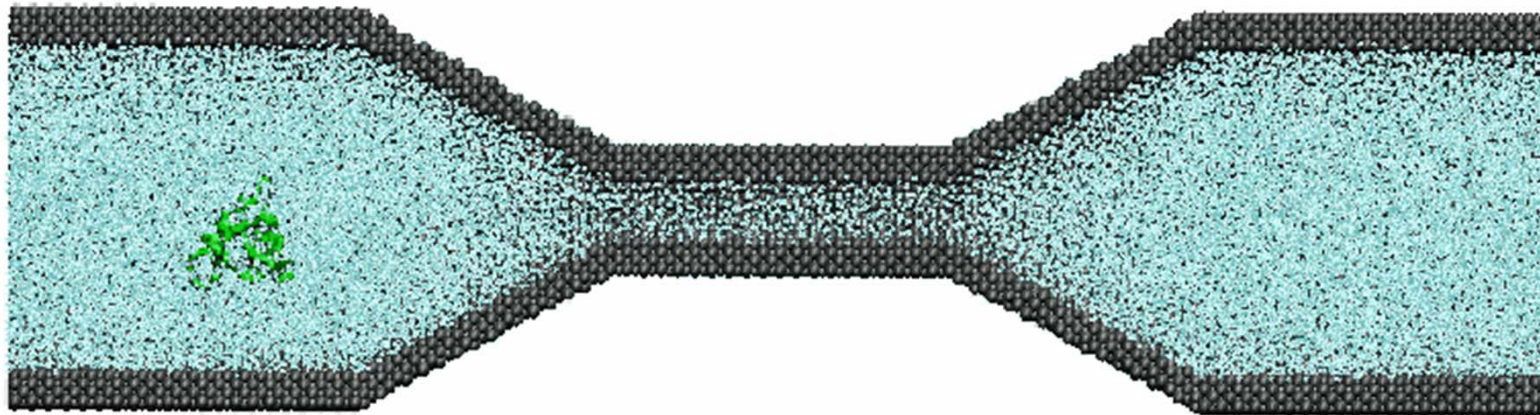


Boundary conditions in DPD

Polymer translocation



Translocation of polymer in single-file conformations



Translocation of polymer in double-folded conformations

Guo, Li, Liu & Liang, J. Chem. Phys., 2011

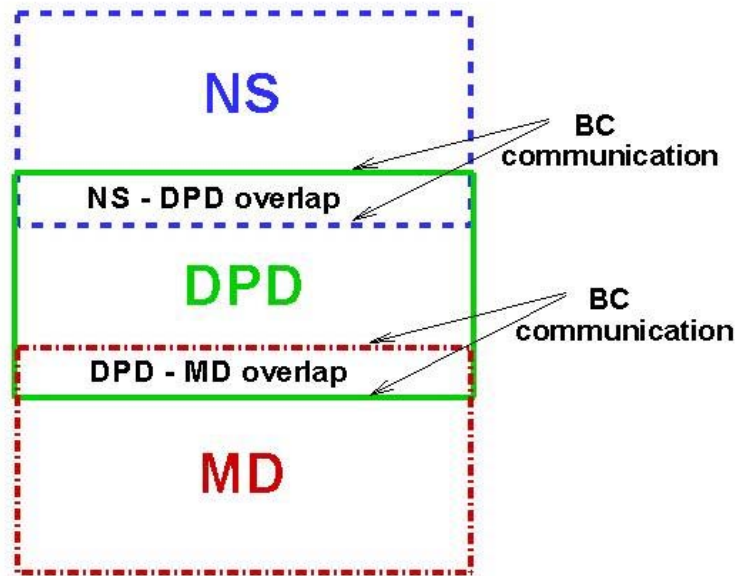


Macro-Meso-Micro Coupling

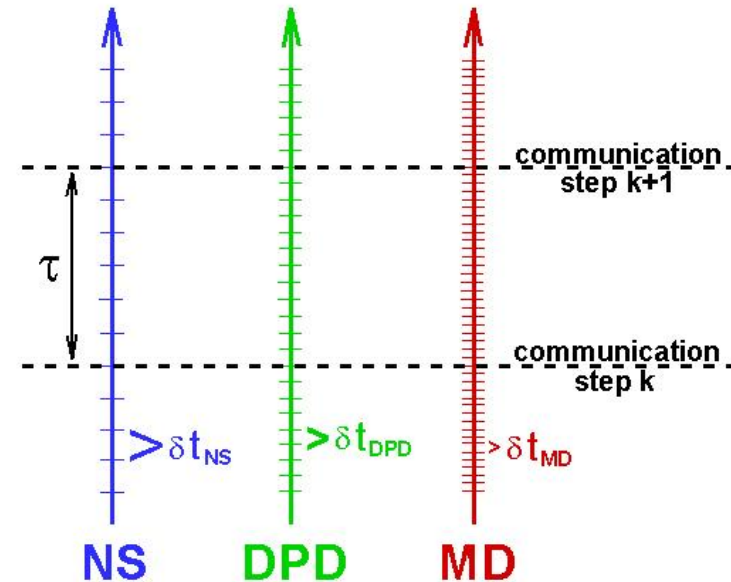
NS + DPD + MD

Triple-Decker Algorithm

Domain decomposition



Time progression

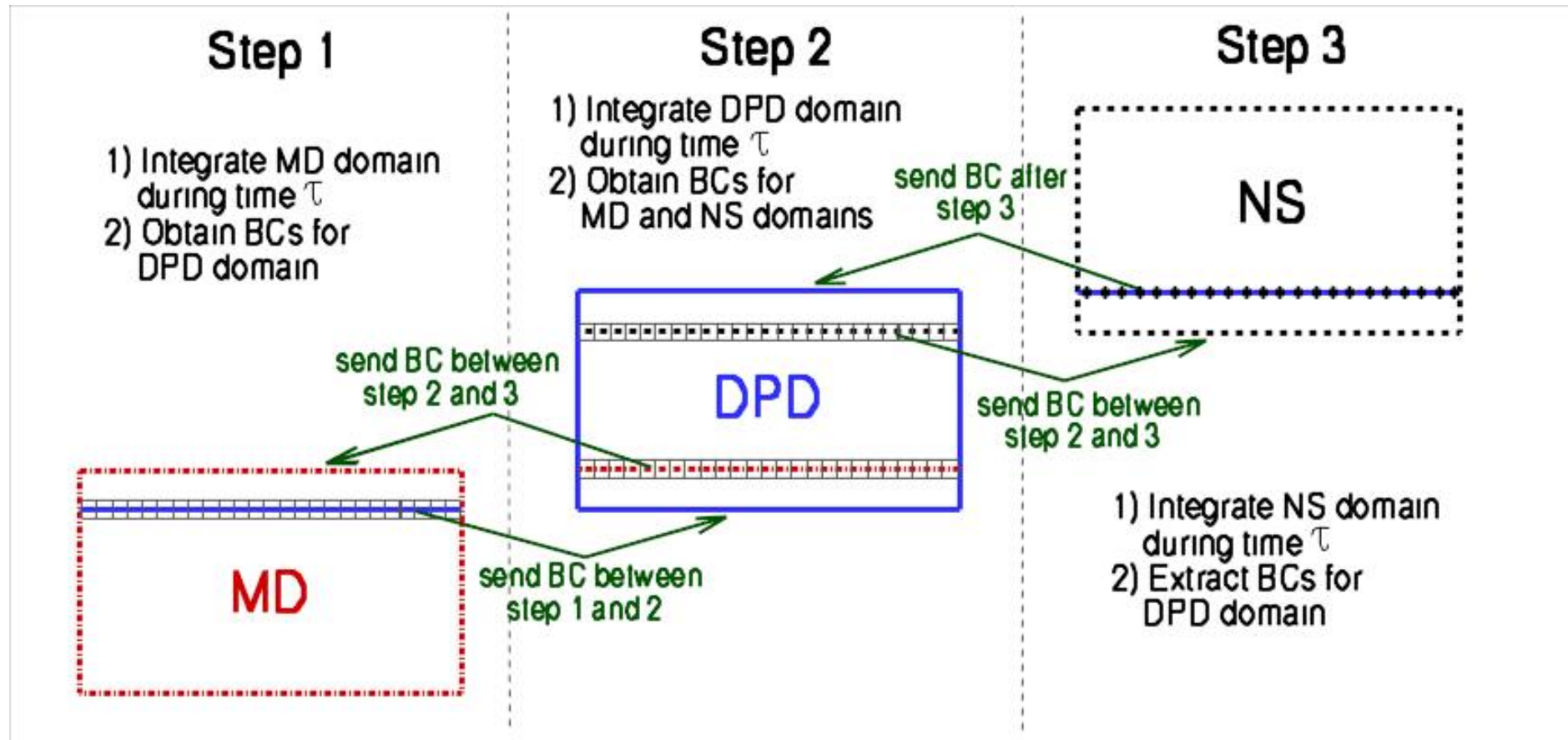


- Atomistic - Mesoscopic - Continuum Coupling
- Efficient time and space decoupling
- Subdomains are integrated independently and are coupled through the boundary conditions every time τ

Fedosov & Karniadakis, J. Comput. Phys., 2009



Triple-Decker Algorithm

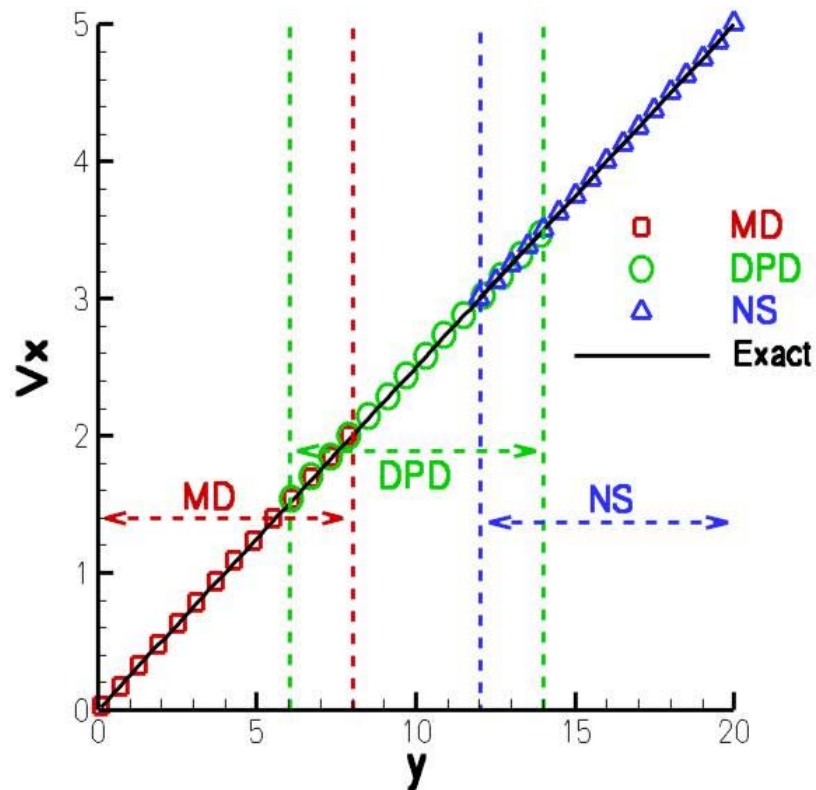


Fedosov & Karniadakis, J. Comput. Phys., 2009

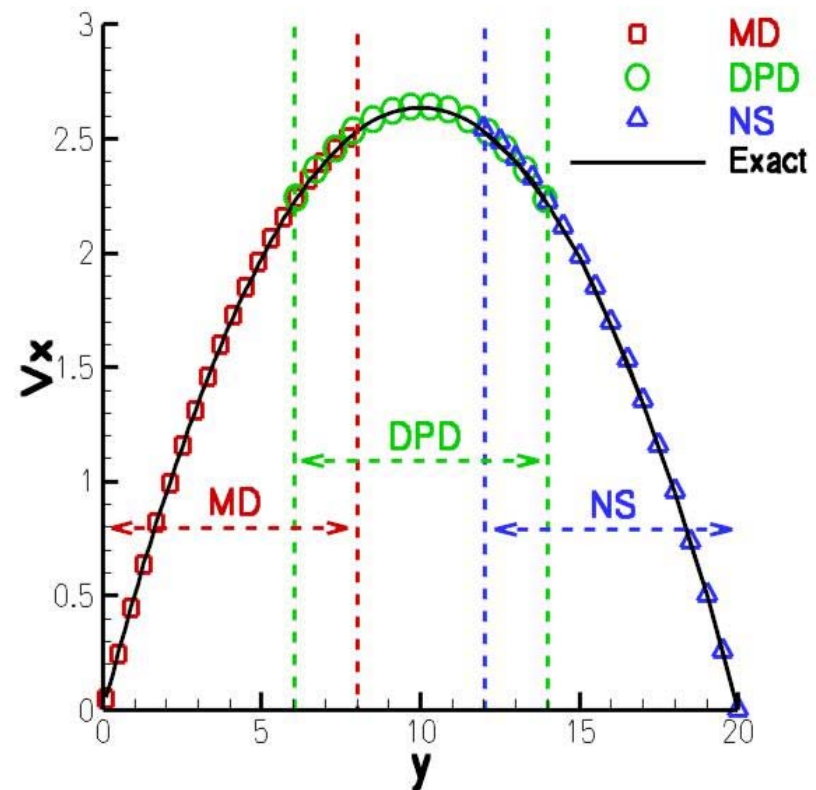


Algorithm validation: 1D flows

Couette flow



Poiseuille flow

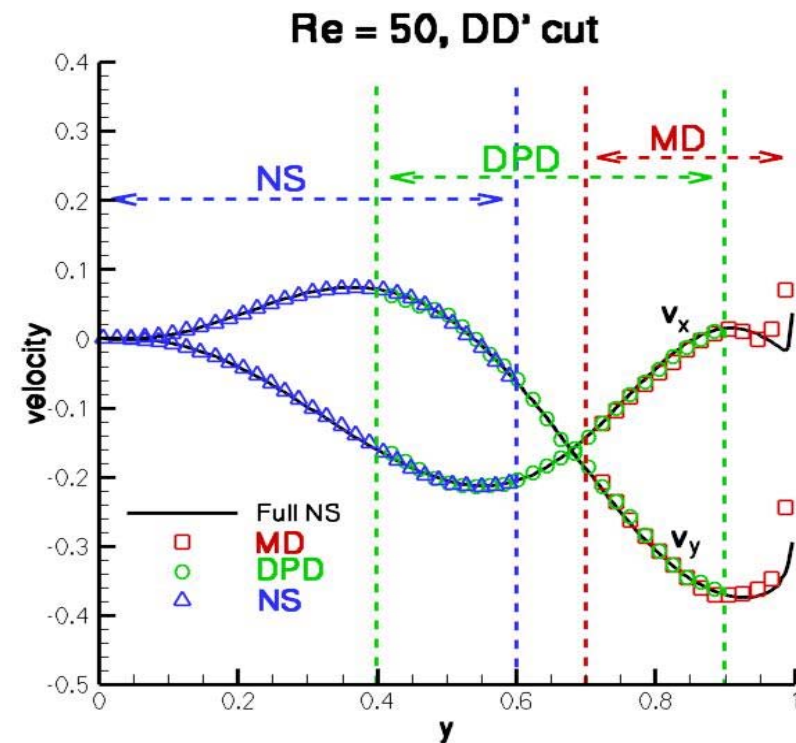
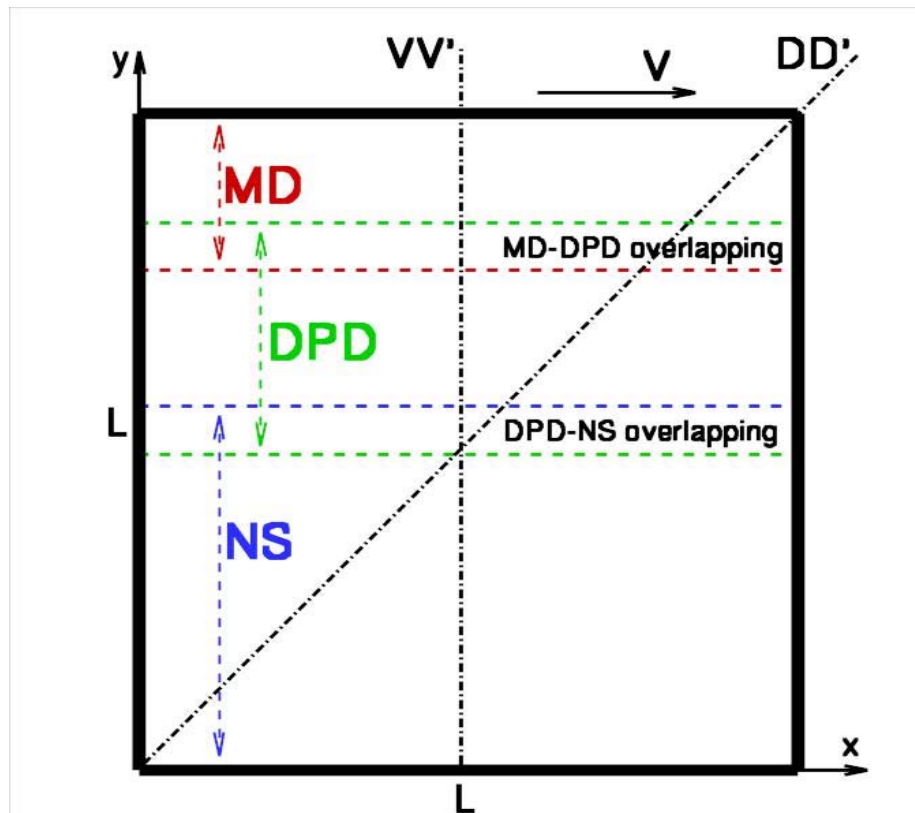


Fedosov & Karniadakis, J. Comput. Phys., 2009



Square cavity flow

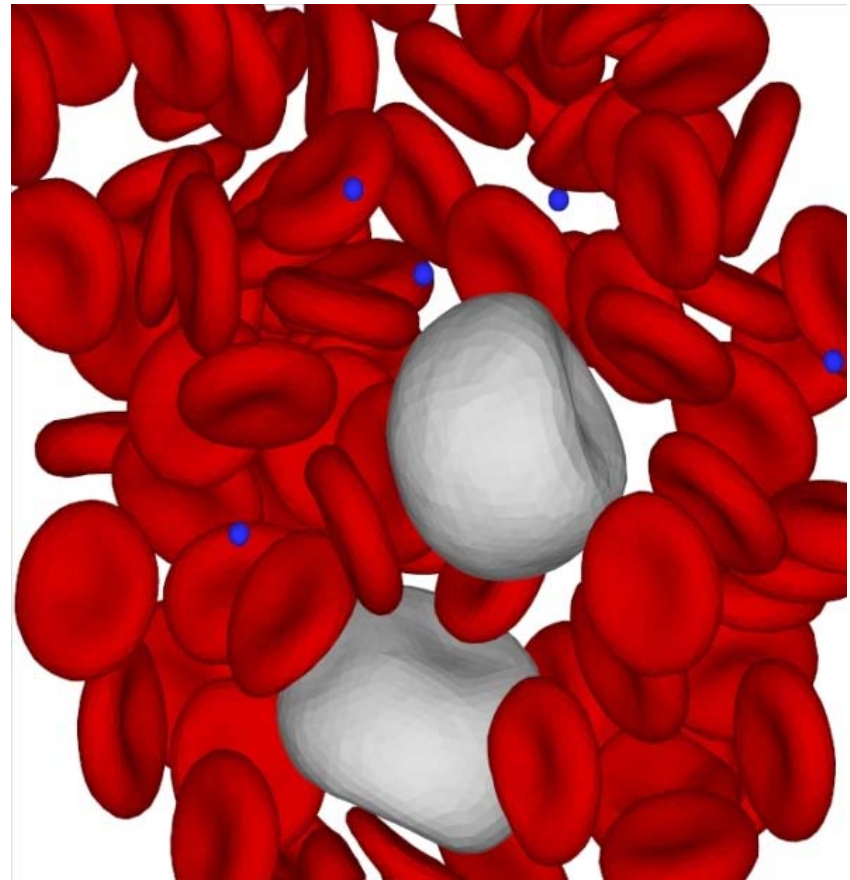
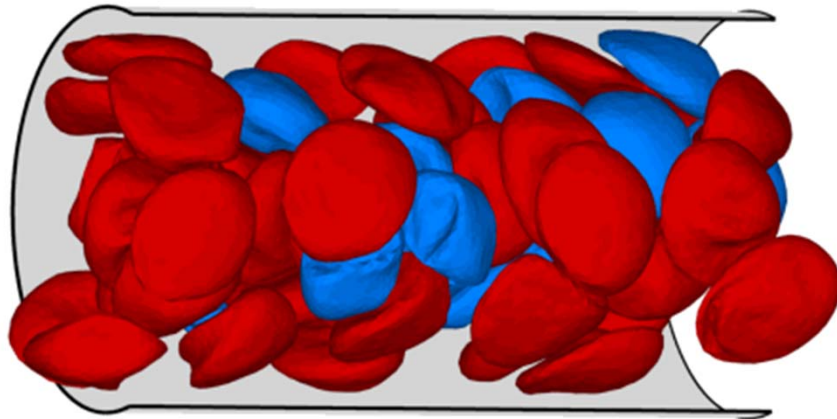
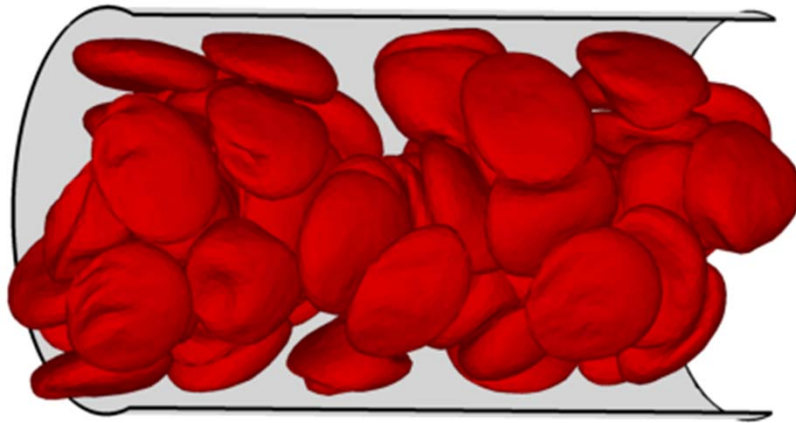
Square cavity, upper wall is moving to the right



Fedosov & Karniadakis, J. Comput. Phys., 2009

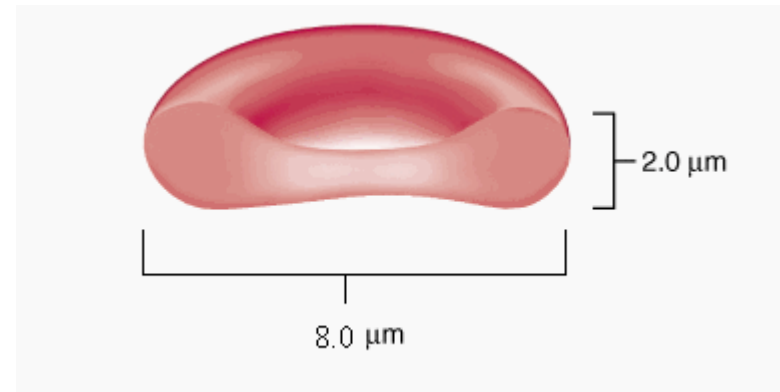
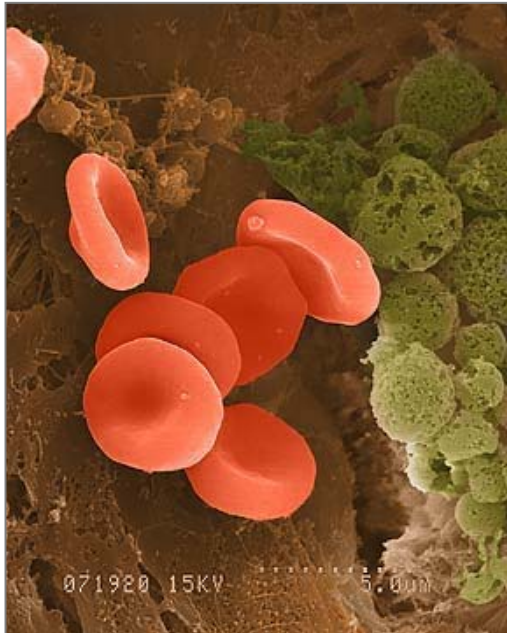


Blood flow

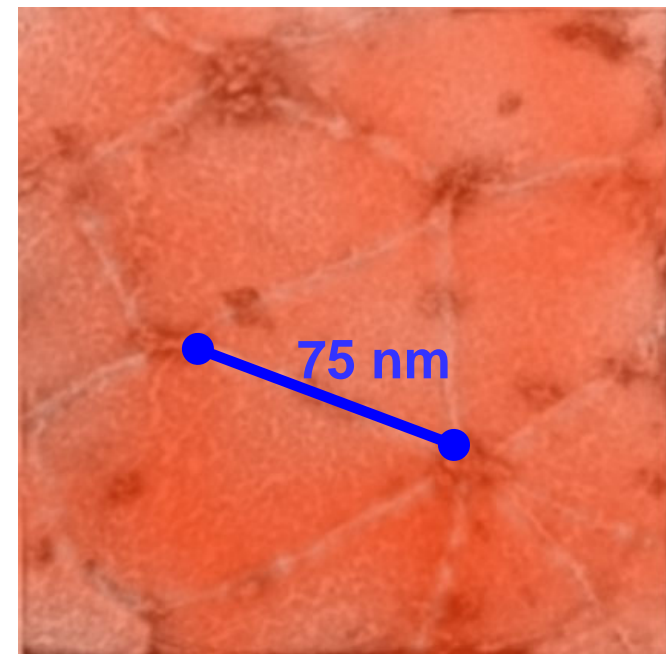
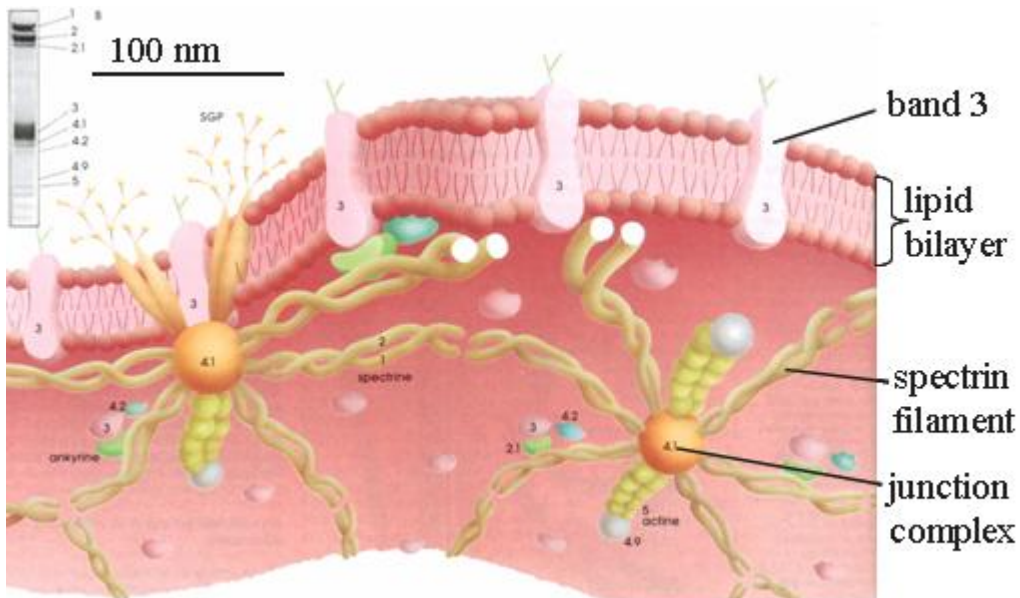


Modeling human blood flow in health and disease

Red Blood Cells



50-100 *nm* spectrin length between junctions
27000 - 40000 of junctions per RBC



General Spectrin-level and Multiscale RBC Models

- ❑ RBCs are immersed into the DPD fluid
- ❑ The RBC particles interact with fluid particles through DPD forces
- ❑ Temperature is controlled using DPD thermostat

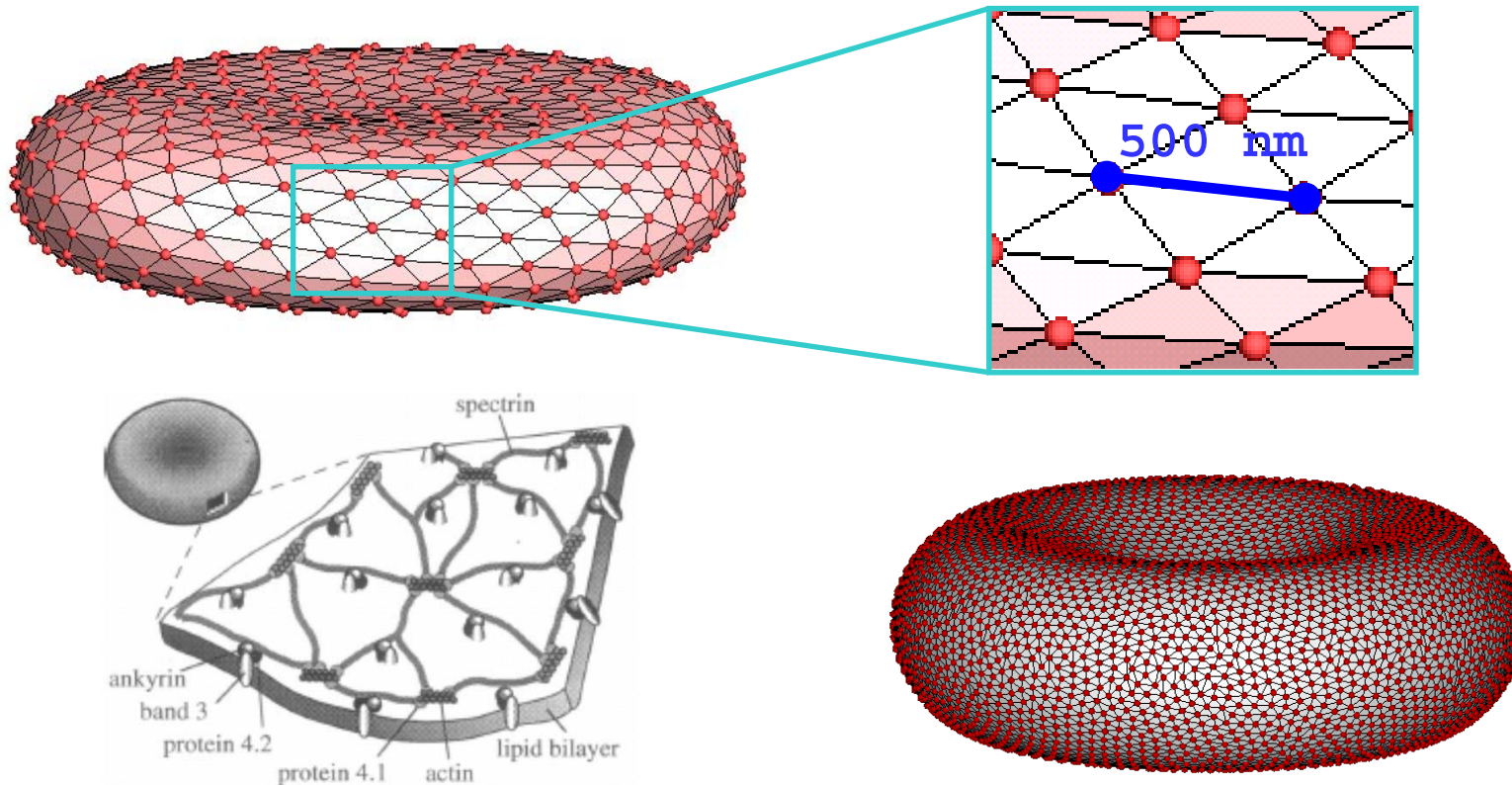


FIGURE 1 Arrangement of the major components of the RBC membrane skeleton.

1. Pivkin & Karniadakis, PRL, 2008;
2. Fedosov, Caswell & Karniadakis, Biophys. J, 2010.

Multiscale RBC model

Triangular mesh:

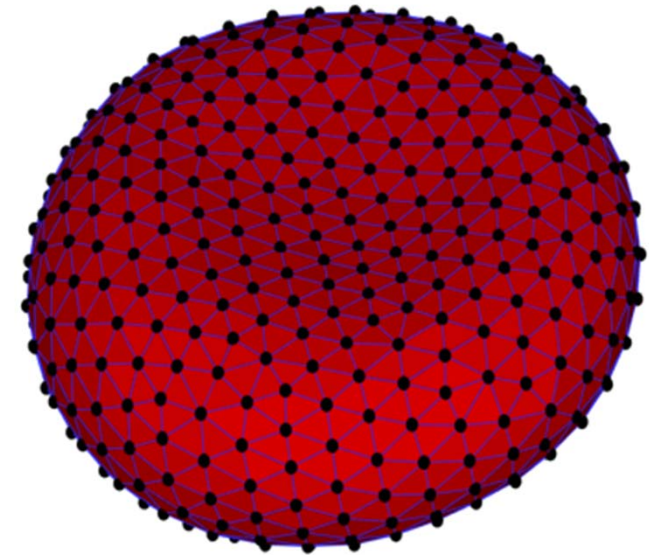
- each vertex - a DPD particle
- each edge - a viscoelastic spring

$$U_{POW-WLC}(x) = \frac{k_p}{(n-1)x^{n-1}} + \frac{k_B T L_m}{4p} \times \frac{3(x/L_m)^2 - 2(x/L_m)^3}{1 - x/L_m} + U_{visc}$$

- bending resistance of lipid bilayer

$$U_{BEND}(\theta_{\alpha\beta}) = k_b [1 - \cos(\theta_{\alpha\beta} - \theta_0)]$$

- shear resistance of cytoskeleton



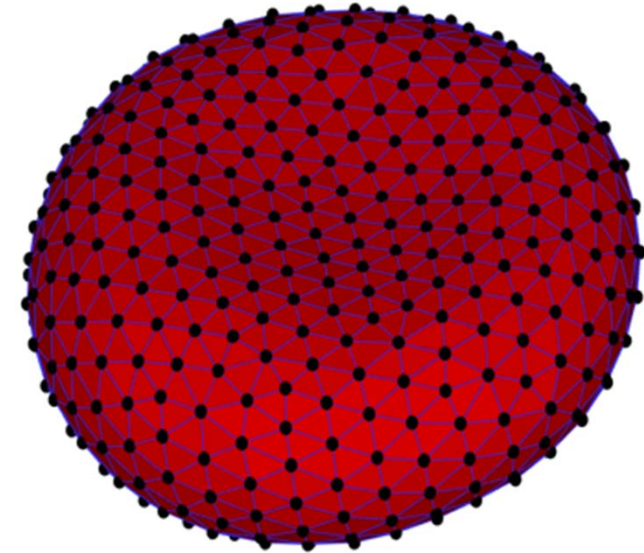
Fedosov, Caswell and Karniadakis. Biophys. J., 2010

Multiscale RBC model

Triangular mesh:

➤ constant surface area

$$U_{AREA}(A) = \frac{k_A(A - A_0^{tot})^2}{2A_0^{tot}} + \sum_{j \in 1 \dots N_f} \frac{k_d(A_j - A_0)^2}{2A_0}$$



➤ constant volume

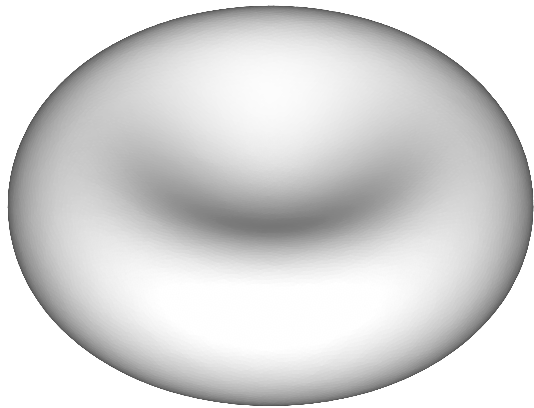
$$U_{VOLUME}(V) = \frac{k_V(V - V_0^{tot})^2}{2V_0^{tot}}$$

Fedosov, Caswell and Karniadakis. Biophys. J., 2010.

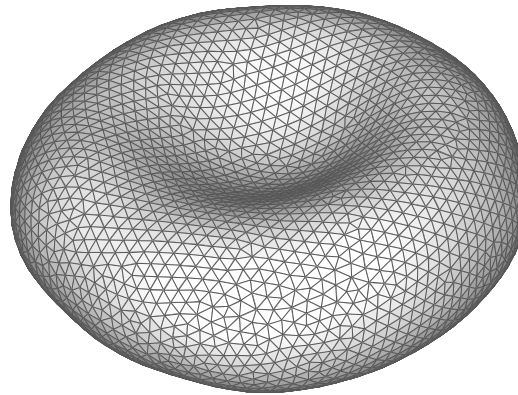
CRUNCH GROUP



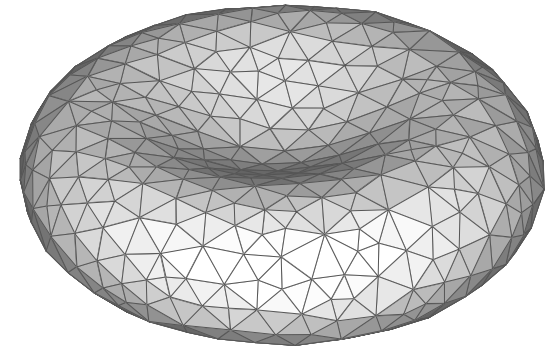
Spectrin-level/Coarse RBC Representation



$N = 27344$



$N = 3000$



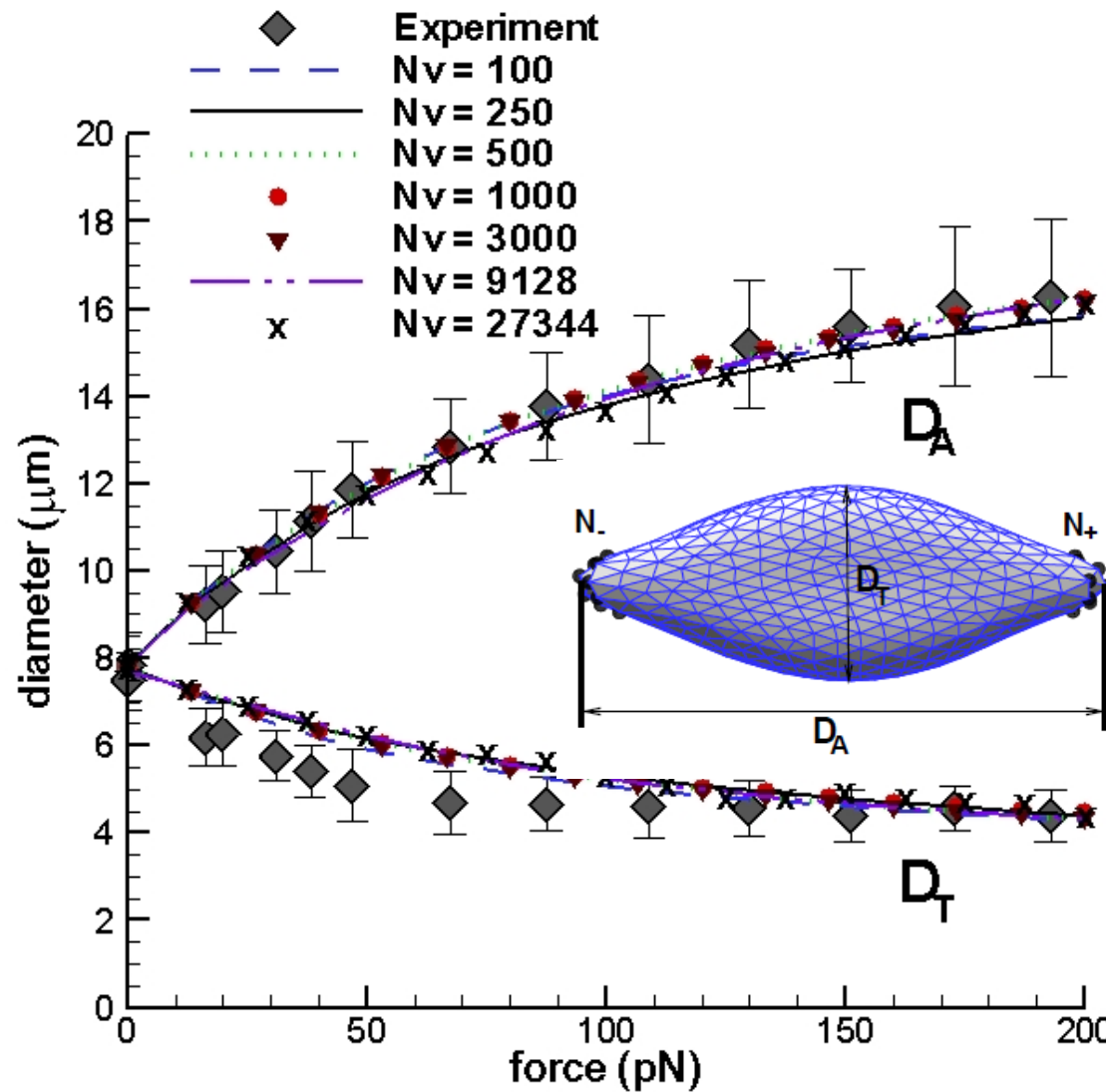
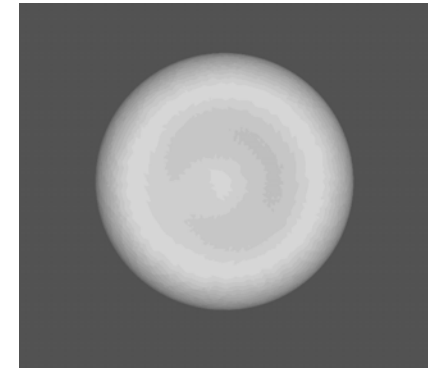
$N = 500$

The membrane macroscopic elastic properties are found analytically for all representations: from spectrin-level to coarse-level.

Pivkin & Karniadakis, PRL, 2008



MS-RBC mechanics: healthy



$$\mu_0 = 6.3 \times 10^{-6} \frac{N}{m}$$

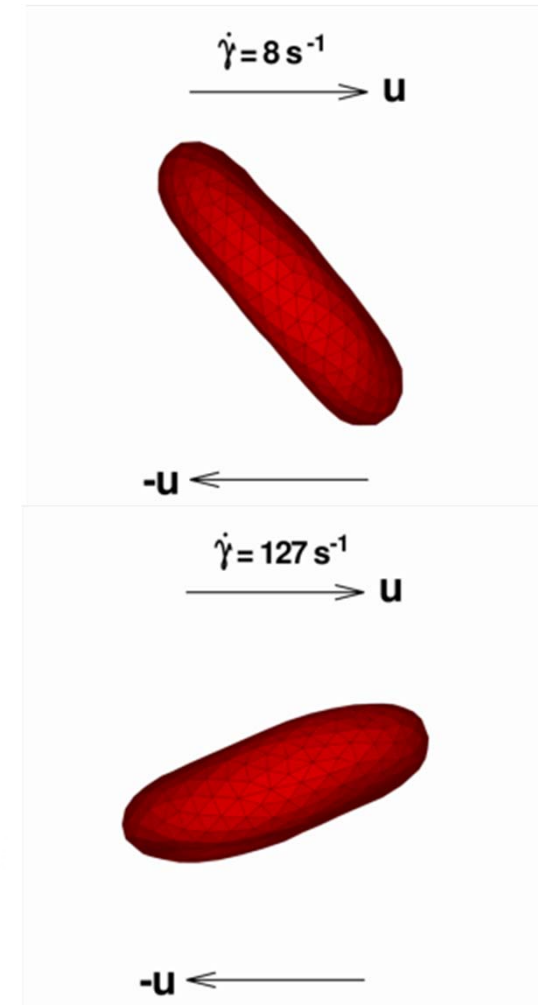
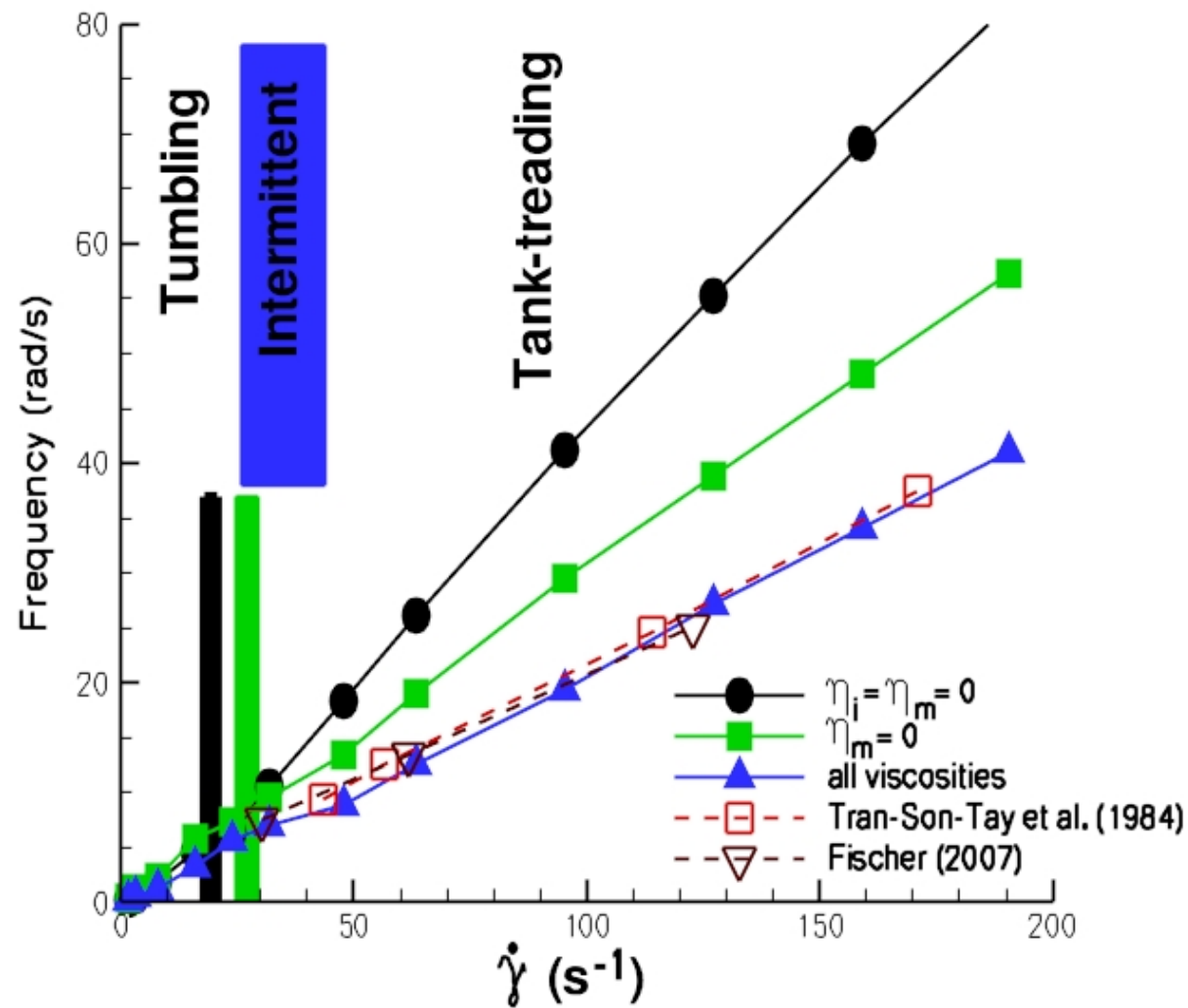
$$Y = 18.9 \times 10^{-6} \frac{N}{m}$$

$$k_c = 2.4 \times 10^{-19} J$$

Experiment - Suresh et al., *Acta Biomaterialia*, 1:15-30, 2005



RBC dynamics in shear flow

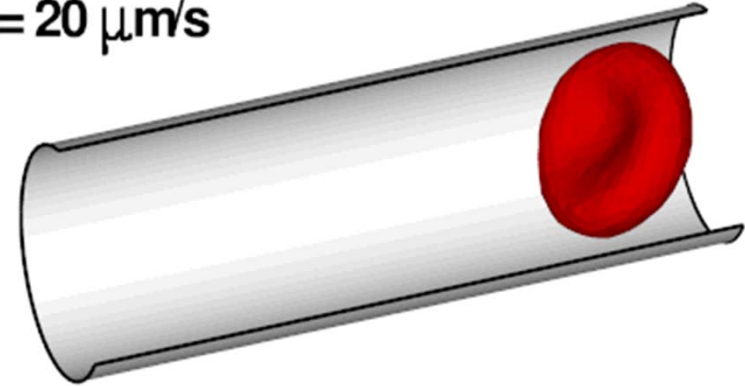


RBC dynamics in Poiseuille flow

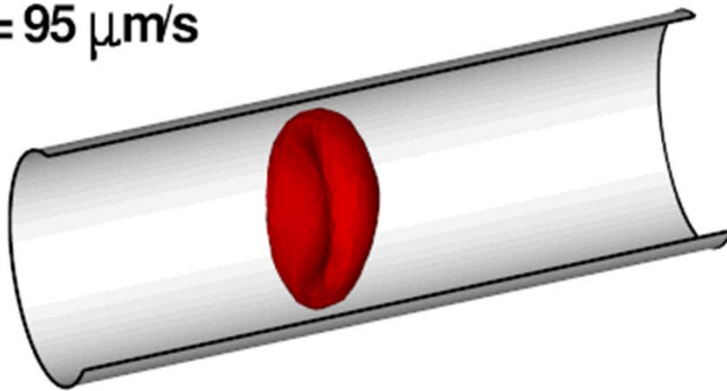
$D = 9 \mu\text{m}$ - tube diameter

$C = 0.05$ - RBC volume fraction

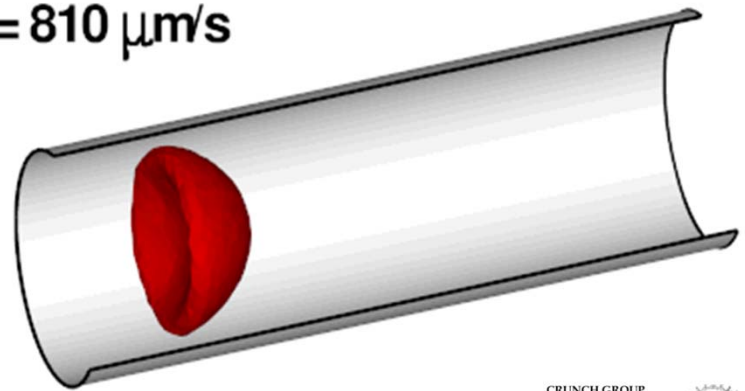
$\bar{U} = 20 \mu\text{m/s}$



$\bar{U} = 95 \mu\text{m/s}$

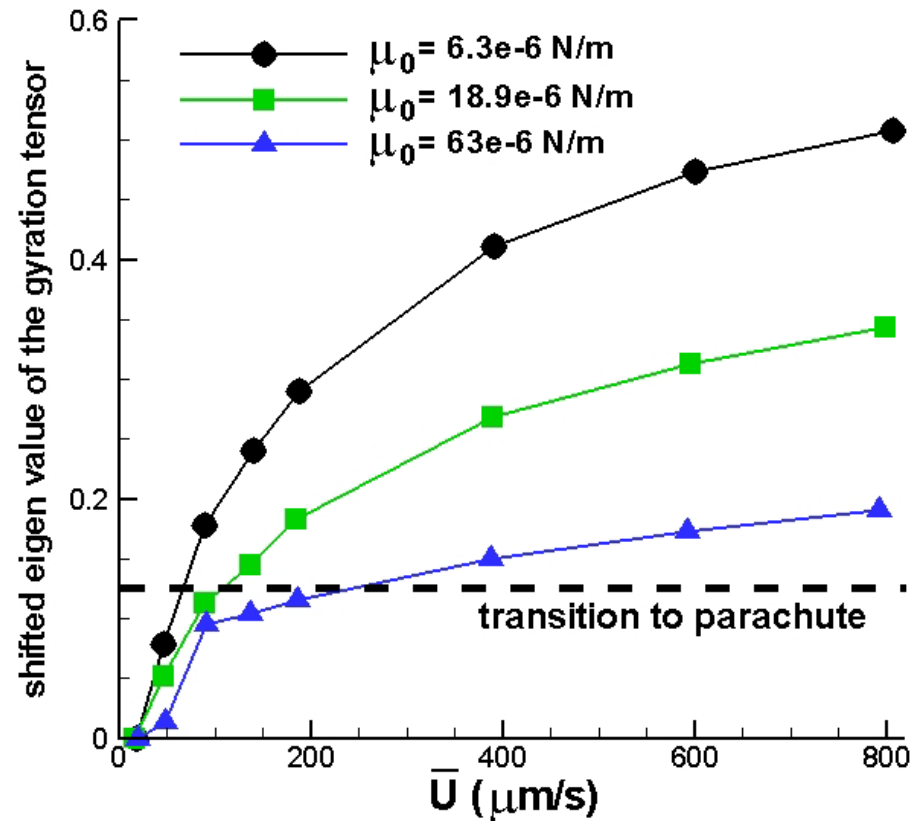
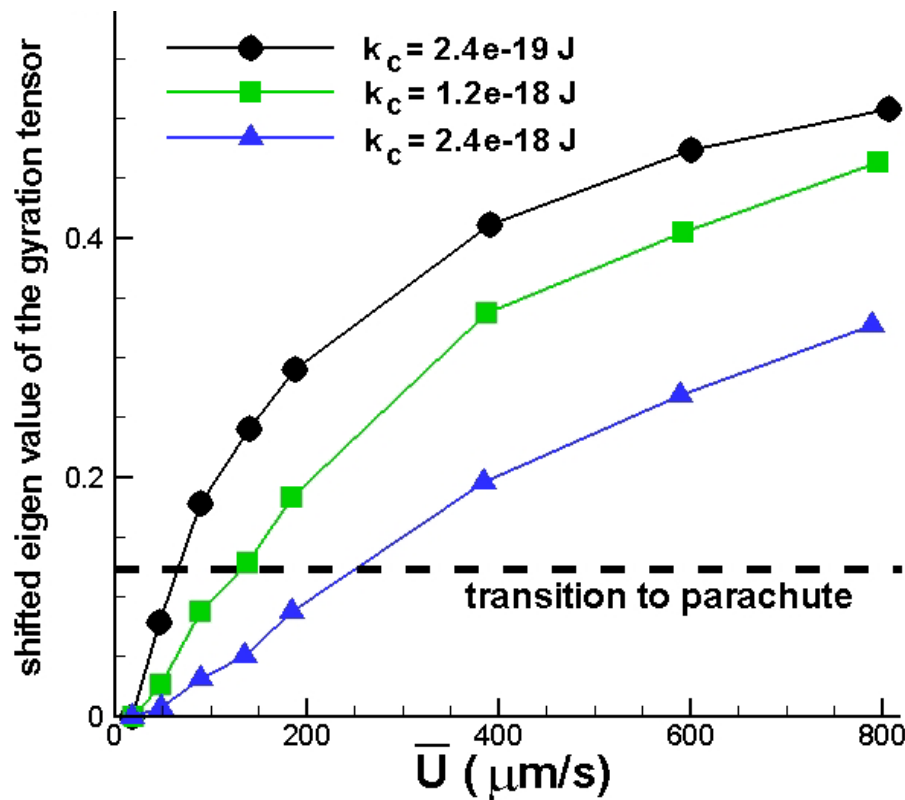


$\bar{U} = 810 \mu\text{m/s}$

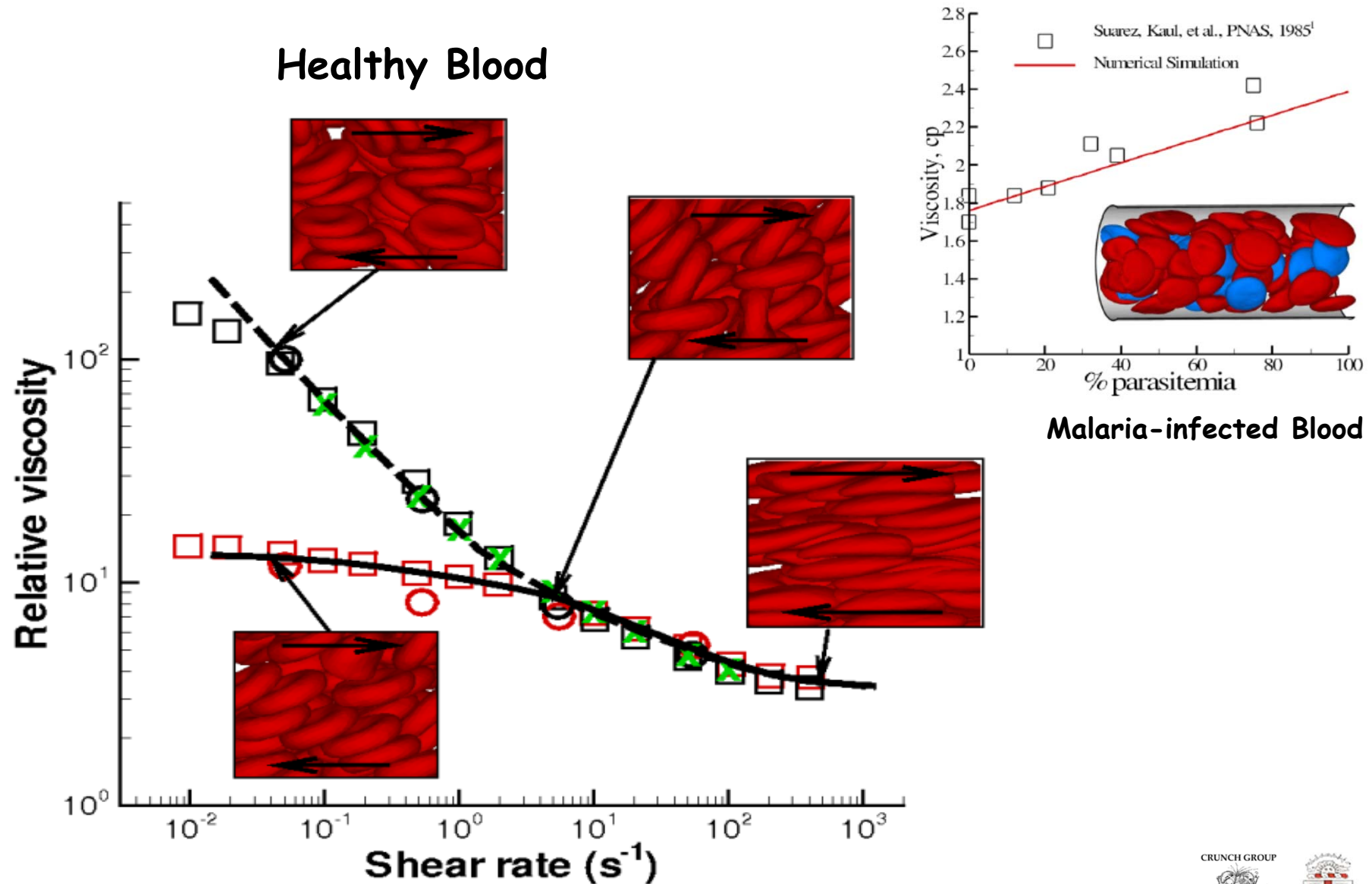


RBC dynamics in Poiseuille flow

$$\bar{U} = \frac{\int v(r) dA}{A} \quad G_{mn} = \frac{1}{N} \sum_i (r_m^i - r_m^{CM})(r_n^i - r_n^{CM}) - \text{gyration tensor}$$



Prediction of Human Blood Viscosity *In Silico*



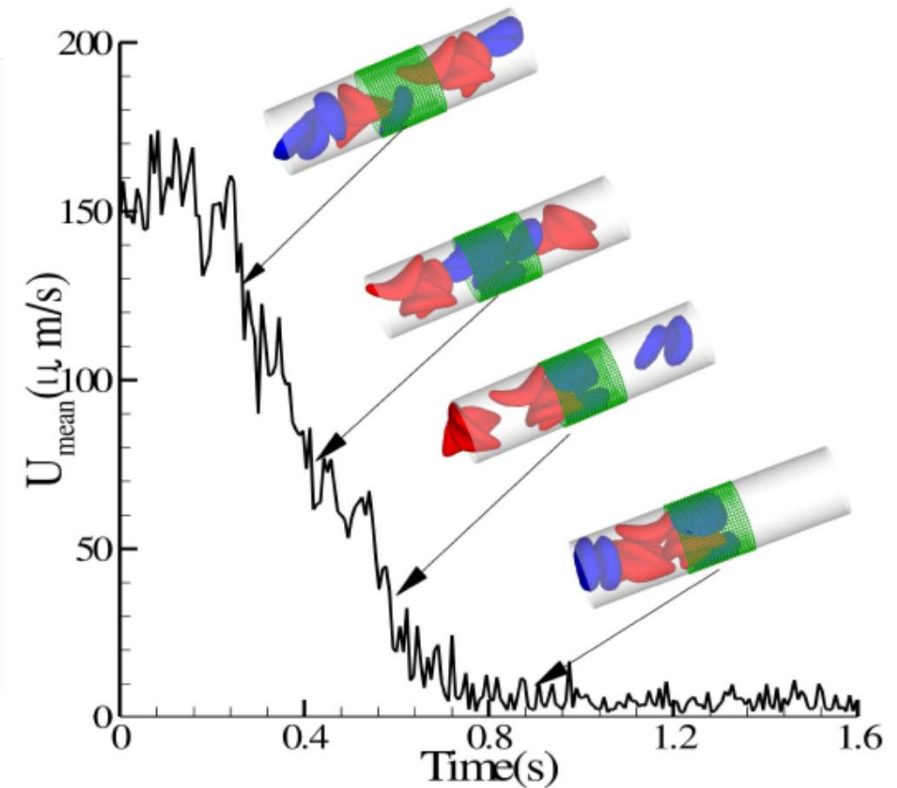
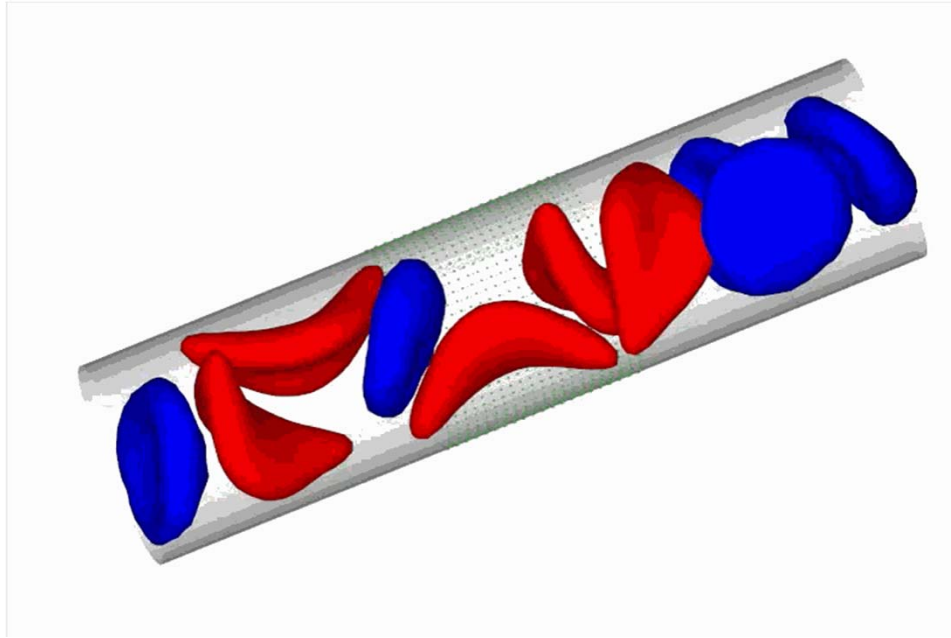
Fedosov, Pan, Caswell, Gompper & Karniadakis, PNAS, 2011

CRUNCH GROUP



Vaso-occlusion in sickle cell disease

Pipe flow (SS2 + SS4)



Deformable SS2 cells
adherent to post capillary

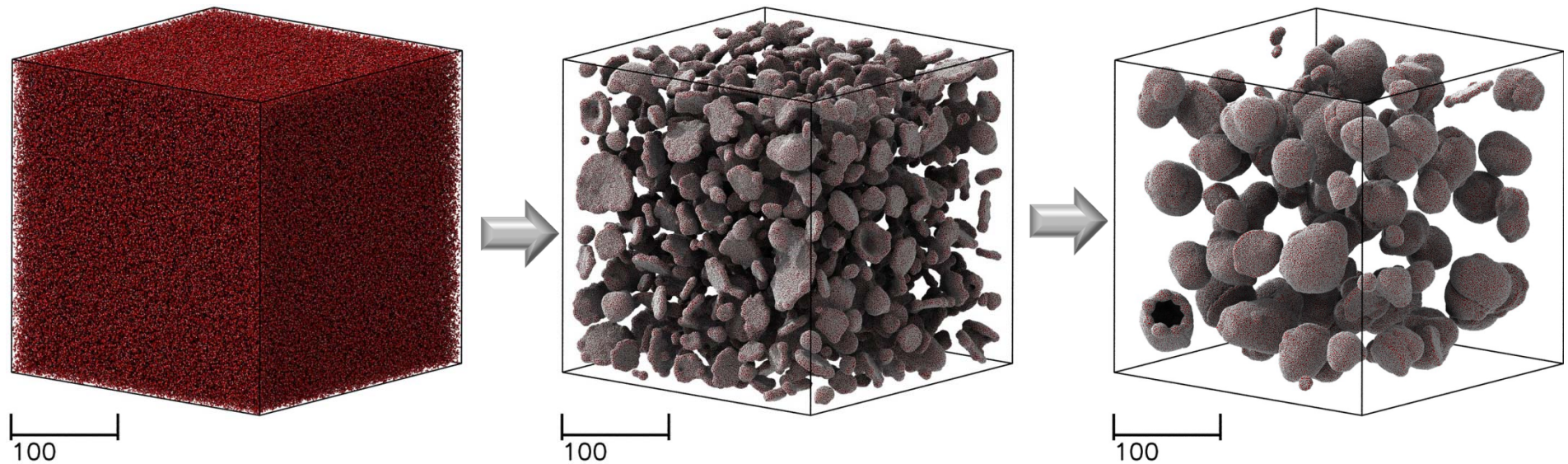
Trap rigid SS4 cells (mostly
Irreversible sickle cells)

Blood occlusion in
post capillary

Lei & Karniadakis, PNAS, 2013

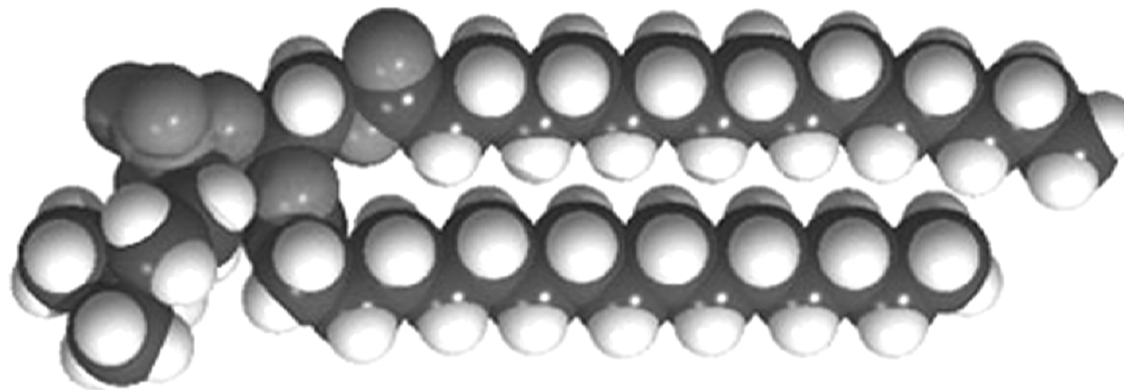
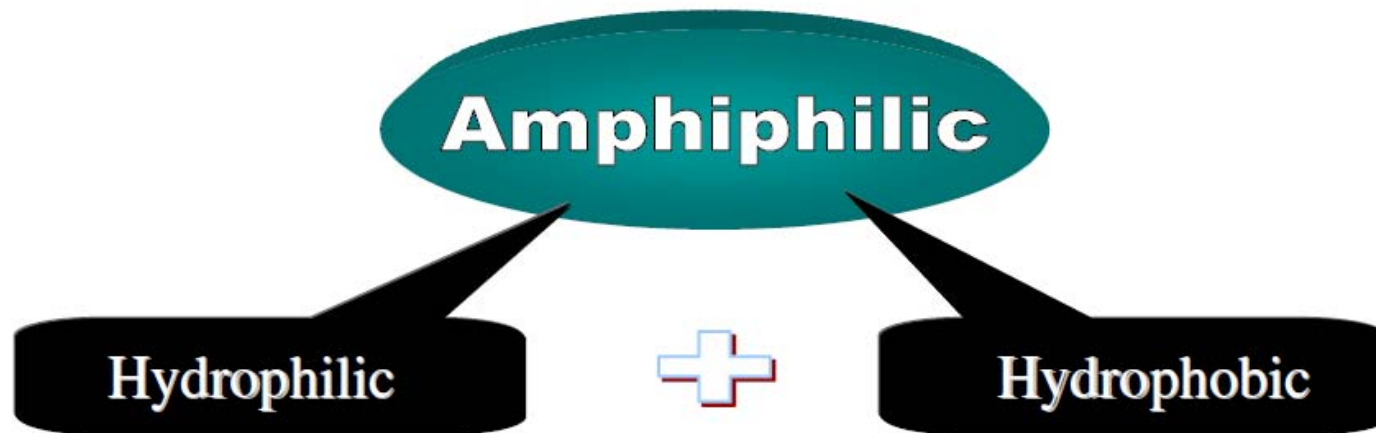


Amphiphilic self-assembly



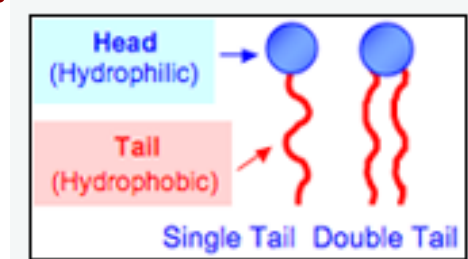
Self-assembled vesicles from **128M** particle simulations

Amphiphilic self-assembly

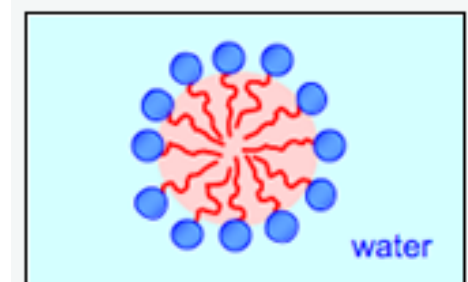


hydrophilic head

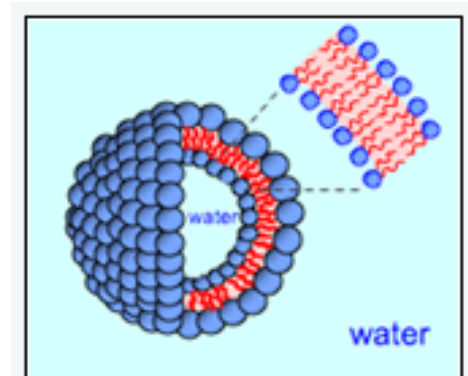
hydrophobic tail



Amphiphilic molecule



Micelle



Vesicle

Amphiphilic self-assembly

DPD repulsion parameter

$$a_{ij} = a_{ii} + \Delta a$$

Hydrophilic and hydrophobic molecules need differences in the repulsion parameters otherwise they would mix

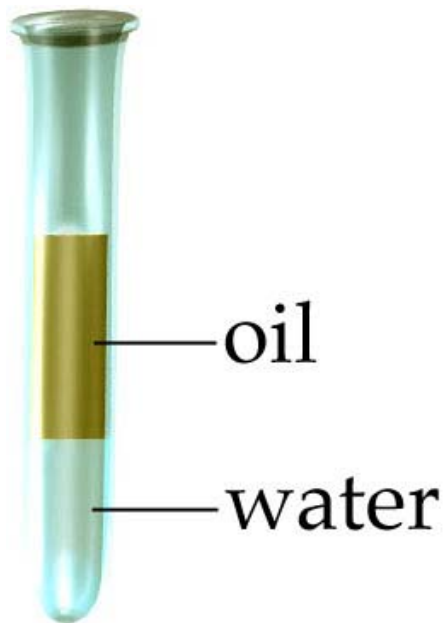
How do we define 'not mixing' and separation ?

Phase separation: mean-field theory

$\chi N < 10.5$ homogeneous or disordered system

$\chi N \cong 10.5$ weak segregation demixing

$\chi N \gg 10.5$ strong segregation demixing

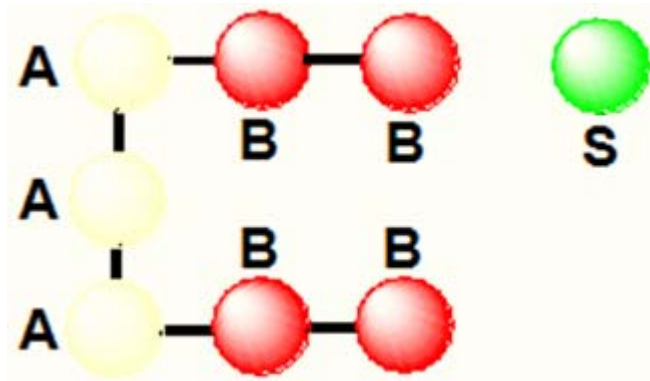


$$\frac{\chi N k_B T}{\Delta a} = 0.306 N \quad [\text{Groot \& Warren (1997)}]$$

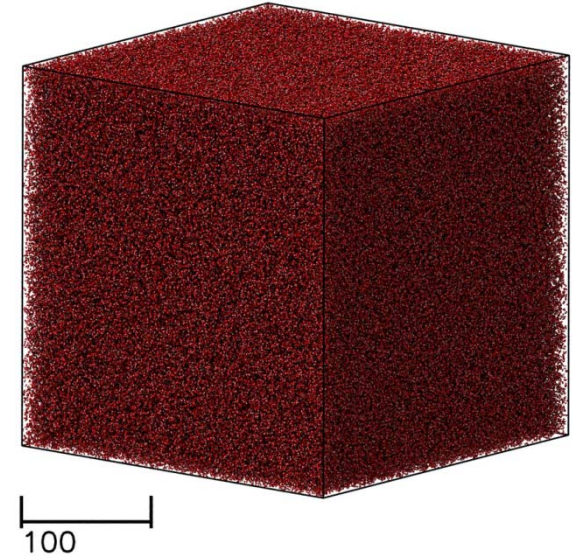


Amphiphilic self-assembly

DPD model



A: hydrophilic
B: hydrophobic
S: solvent



Particle density: $\rho = 5$; Polymer length: $N = 7$

DPD parameters

Two alike particles
(A-A, B-B, S-S, A-S)

$$a_{ii} = 75 \frac{k_B T}{\rho r_c^4}$$



$$a_{ii} = 15$$

Two unlike particles
(A-B, B-S)

$$a_{ij} = a_{ii} + \Delta a$$

$$\frac{\chi N k_B T}{\Delta a} = 0.306 N$$

$$\chi N \sim 32.1$$

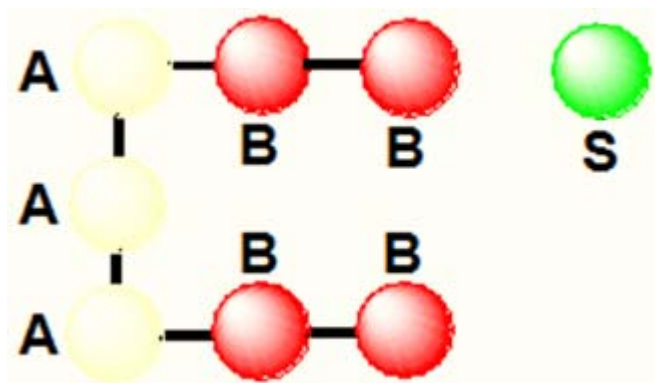
strong segregation regime

$$a_{ij} = 120$$

CRUNCH GROUP



Amphiphilic self-assembly



A: hydrophilic

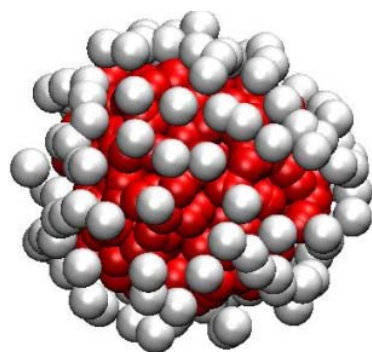
B: hydrophobic

S: solvent

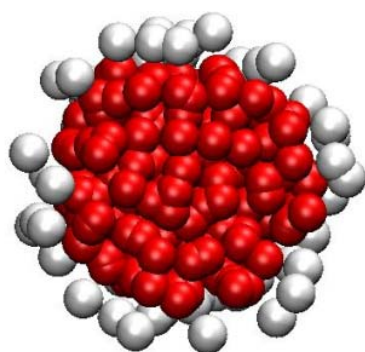
Repulsive parameters:

$$a_{ij} = \begin{pmatrix} & A & B & S \\ A & 15 & 120 & 15 \\ B & 120 & 15 & 120 \\ S & 15 & 120 & 15 \end{pmatrix}$$

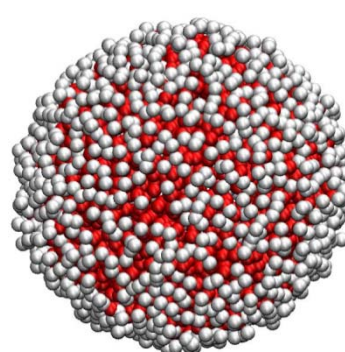
Self-assembled microstructures:



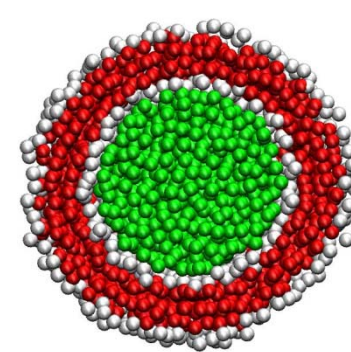
spherical micelle



slice



vesicle



slice

Li, Tang, Liang & Karniadakis, Chem Commun, 2014



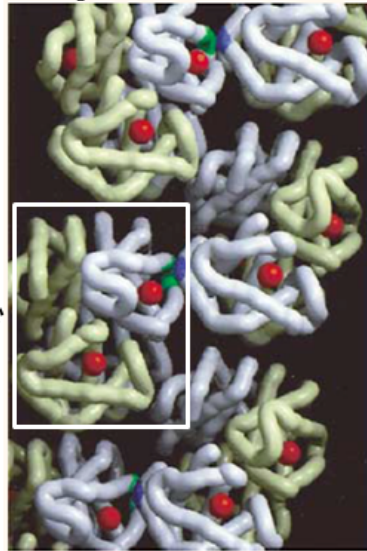
Chirality controls molecular self-assembly

HbS molecule (MW: ~ 67,000 Da)

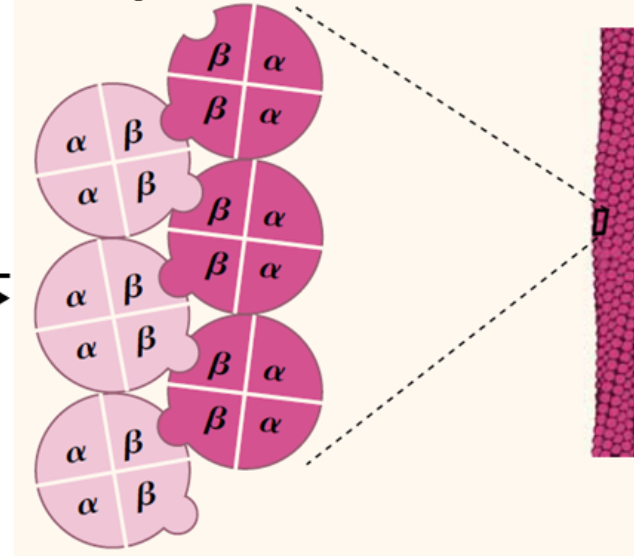


HbS polymerizes into filaments

High-resolution model

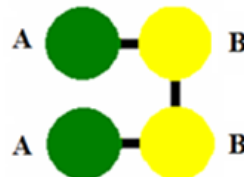


Coarse-grained model

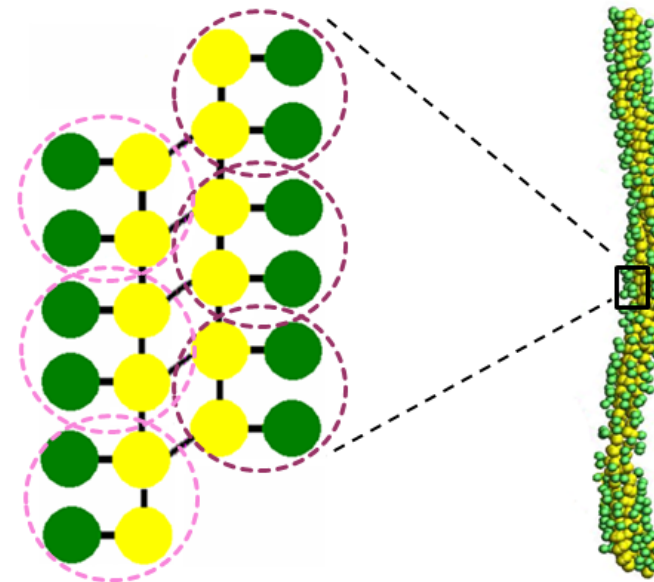


Polymer fiber

Coarse-graining



Polymerization



Sickle hemoglobin (HbS)



Chirality controls molecular self-assembly

DPD interactions:

$$V_{\text{tot}} = V_{\text{bonded}} + V_{\text{nonbonded}} = (V_{\text{str}} + V_{\text{bend}} + V_{\text{tors}}) + (V_{\text{vdw}} + V_{\text{es}} + \dots)$$

Bonded interactions:

Hookean spring interaction:

$$V_{\text{str}} = k_{\text{str}} (r - r_0)^2$$

Bond-bending interaction:

$$V_{\text{bend}} = k_{\text{bend}} (\theta - \theta_0)^2$$

Bending FENE interaction:

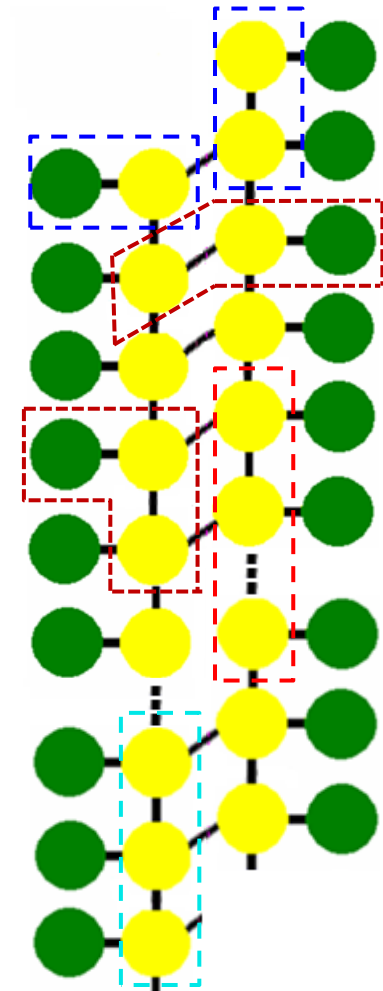
$$F_{\text{FENE}} = k_{\text{BEND}} \left[\frac{\theta - \theta_0}{1 - (\theta - \theta_0) / \Delta\theta_{\text{max}}} \right] \quad (c)$$

Non-bonded interactions:

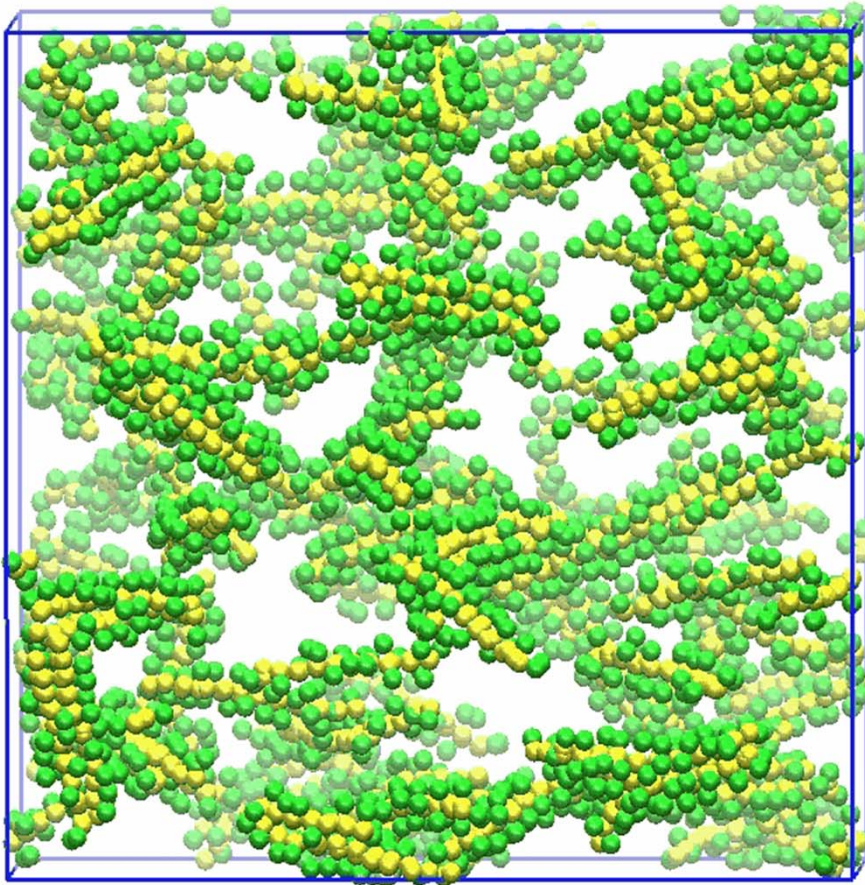
Pairwise DPD conservative interaction:

$$V_{\text{non-bonded}} = -\frac{a_{ij}}{2} \left(1 - r_{ij} / r_c \right)^2$$

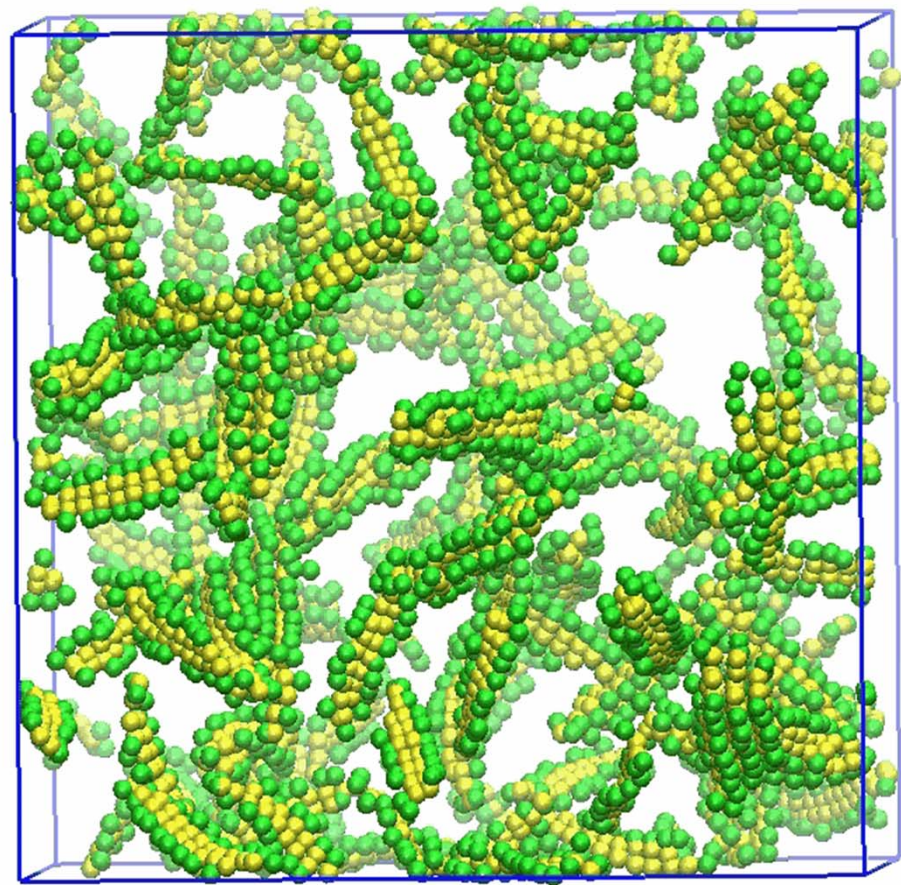
(a) } Control chain rigidity
(b1) }
(b2) } Describe chain chirality
(c) }



Chirality controls molecular self-assembly



Elongated step-like fiber



Elongated sheet-like membrane

Li, Caswell & Karniadakis, Biophys. J., 2012

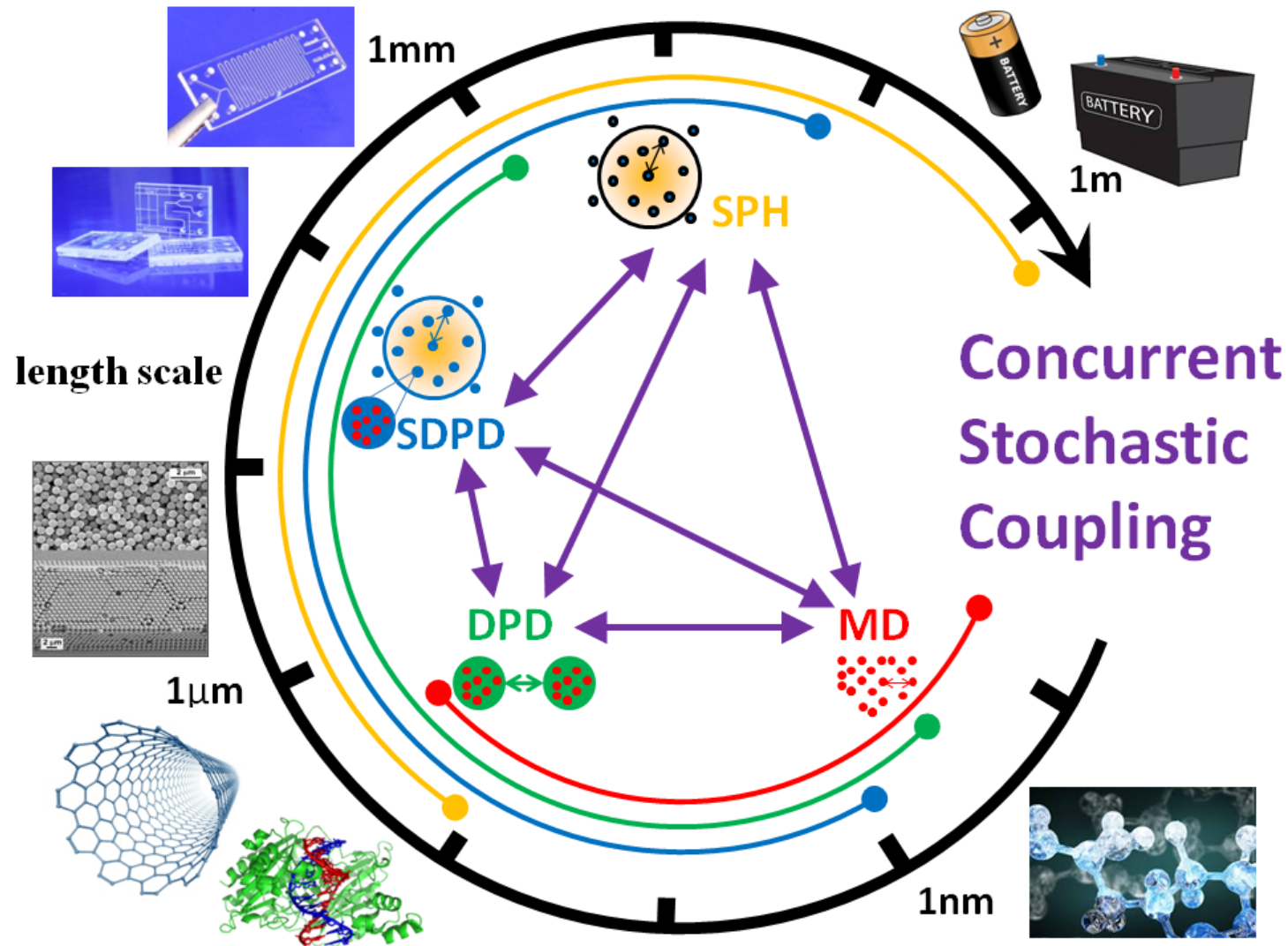
Summary

Dissipative Particle Dynamics is a powerful tool to

- treat boundary conditions in microchannel flows
- simulate the dynamic and rheological properties of simple and complex fluids
- understand the dynamic behavior of polymer and DNA chains
- model blood flow in health and disease

The future of DPD

- Multiscale modeling: MD - DPD - SDPD - SPH



The future of DPD

- Complex fluids and complex geometries
- Parameterization development for simulating real fluids
- Structural models

References

1. Boek, Coveney, Lekkerkerker & van der Schoot. Simulating the rheology of dense colloidal suspensions using dissipative particle dynamics. *Phys. Rev. E*, 1997, 55, 3124.
2. Groot & Warren. Dissipative particle dynamics: Bridging the gap between atomistic and mesoscopic simulation. *J. Chem. Phys.*, 1997, 107, 4423.
3. Fan, Phan-Thien, Yong, Wu & Xu. Microchannel flow of a macromolecular suspension. *Phys. Fluids*, 2003, 15, 11.
4. Pivkin & Karniadakis. Controlling density fluctuations in wall-bounded dissipative particle dynamics systems. *Phys. Rev. Lett.*, 2006, 96, 206001.
5. Pivkin & Karniadakis. Accurate coarse-grained modeling of red blood cells. *Phys. Rev. Lett.*, 2008, 101, 118105.
6. Fedosov & Karniadakis. Triple-decker: Interfacing atomistic-mesoscopic-continuum flow regimes. *J. Comput. Phys.*, 2009, 228, 1157.
7. Fedosov, Caswell & Karniadakis. A multiscale red blood cell model with mechanics, rheology, and dynamics. *Biophys. J.*, 2010, 98, 2215.



References

8. Fedosov, Pan, Caswell, Gompper & Karniadakis. Predicting human blood viscosity in silico. PNAS, 2011, 108, 11772.
9. Groot & Rabone. Mesoscopic simulation of cell membrane damage, morphology change and rupture by nonionic surfactants. Biophys. J., 2001, 81, 725.
10. Guo, Li, Liu & Liang. Flow-induced translocation of polymers through a fluidic channel: A dissipative particle dynamics simulation study. J. Chem. Phys., 2011, 134, 134906.
11. Lei & Karniadakis. Probing vasoocclusion phenomena in sickle cell anemia via mesoscopic simulations. PNAS, 2013, 110, 11326.